

1 Receptor cavity-based screening reveals potential
2 allosteric modulators of gonadotropin receptors in
3 carp (*Cyprinus carpio*)

4
5 *Ishwar Atre, Lian Hollander-Cohen, Hodaya Lankry, Berta Levavi-Sivan**
6 Department of Animal Sciences, The Robert H. Smith Faculty of Agriculture, Food, and
7 Environment, Hebrew University of Jerusalem, Rehovot 76100, Israel.

8 *Corresponding Author: Berta Levavi-Sivan*

9 E-mail: berta.sivan@mail.huji.ac.il

10

11

12
13

14 **Keywords:**
15 Follicle Stimulating Hormone Receptor; luteinizing hormone receptor; receptor cavity based
16 virtual screening; allosteric modulators; small compound agonists

17 **Abstract**

18 The gonadotropins follicle stimulating hormone (FSH) and luteinizing hormone (LH) are key
19 regulators of sexual development and the reproductive cycle in vertebrates. Unlike most G protein-
20 coupled receptors (GPCR), the FSHR and LHR have large extracellular domains containing
21 multiple leucine-rich repeats, which leads to an elaborate mechanism of receptor activation via
22 orthosteric sites that is difficult to manipulate synthetically. To bypass the orthosteric mechanism,
23 in this study using carp as a model organism we identified allosteric sites capable of receptor
24 activation on the transmembrane domain, which are spatially separated from the orthosteric sites.
25 We have further generated pharmacophore hypothesis based on the structural motifs and exposed
26 residues of these cavities. Using available online small compound libraries consisting of >70000
27 small molecules, we have thereon used receptor cavity-based hypothesis and other screening stages
28 to identify potential modulators of the allosteric binding site on the carp FSHR and LHR *in-silico*.
29 We then examined by *in vitro* transactivation assay the effect of four candidate compounds on
30 FSHR and LHR, as compared to the activity of native ligands. Our results reveal both specific and
31 dual effective allosteric modulators for FSHR and LHR, demonstrating the potential of our
32 approach for efficient pharmacophore-based screening.

33

34

35

36

37

38 **Introduction**

39 In vertebrates, the growth and activity of the gonads is regulated by two gonadotropins hormones
40 (GTH): follicle-stimulating hormone (FSH) and the luteinizing hormone (LH). These
41 hypophysiotropic hormones, belong to the glycoprotein family and play distinctive roles in
42 reproduction. While FSH is responsible for gametogenesis and sustenance of ovarian follicles in
43 females and sperm in males, LH is responsible for gamete maturation in both sexes and ovulation
44 in females ^{1,2}. Both aquaculture and conservation depend on GTH hormones to regulate a species'
45 reproductive cycle for successful breeding and survival. However, in the absence of the natural
46 ecosystems and environmental niches, hormonal secretion patterns affecting the reproductive cycle
47 are perturbed, raising the need for synthetic manipulations of hormonal activity, by artificial
48 molecular tools.

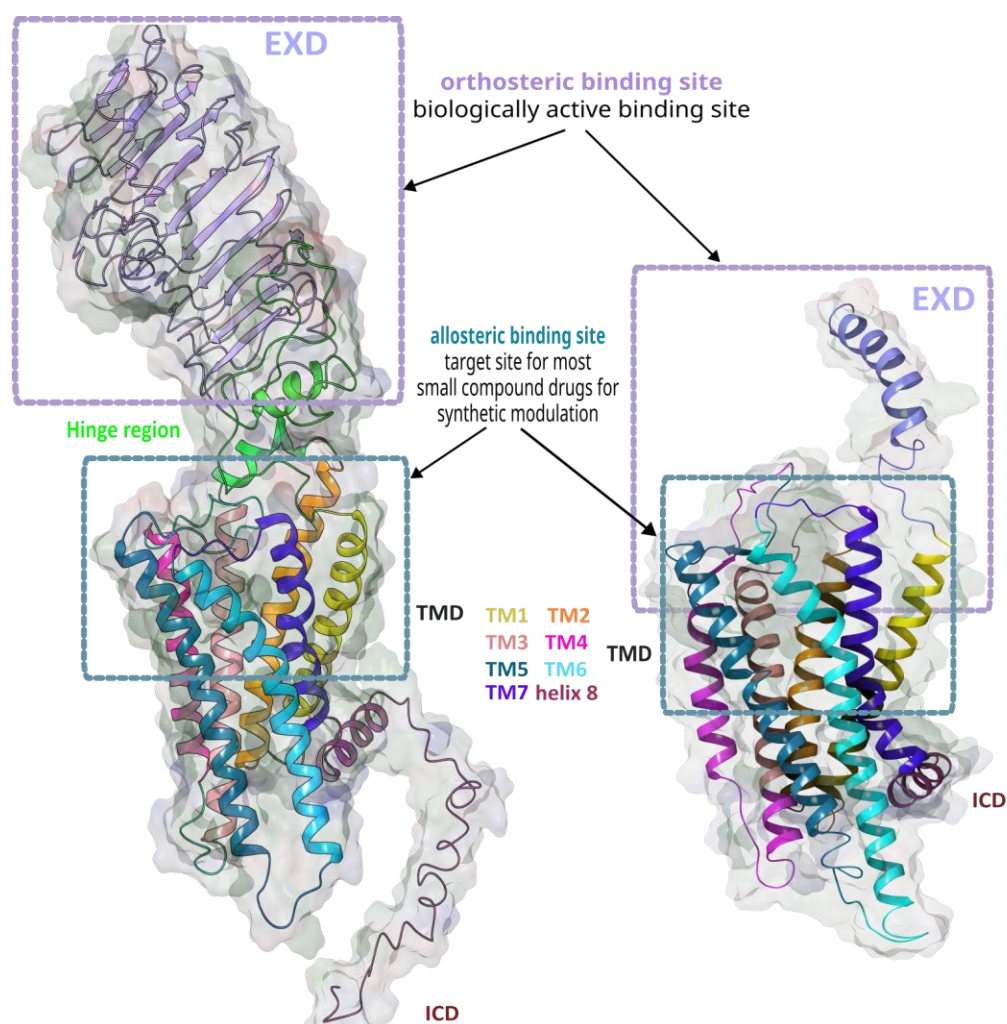
49 LH and FSH are heterodimers composed of a common glycoprotein α -subunit non-covalently
50 attached to a unique β -subunit ³. These α - β complexes bind to gonadotropin receptors (GTHRs),
51 which belong to the G protein-coupled receptor (GPCR) super family, to further influence the
52 progression of gonadal development and sexual maturation. In mammals, knockout or
53 dysfunctionality of GTHRs cause infertility and other complications related to vertebrate
54 reproductive cycles, such as Hypogonadotropic hypogonadism and premature or delayed puberty,
55 infertility, etc. ⁴. A majority of these dysfunctions can be overcome by synthetic or
56 pharmacological stimulation of the receptor in question. In fish, loss of function of FSHR causes
57 masculinization and suppression of ovarian development in female medaka, whereas LHR
58 knockouts were observed to stop ovulation ^{5,6}. Recent studies leveraging advances in in silico
59 methods and the availability of whole-crystal structures of GTHRs ^{7,8} have greatly increased our
60 understanding of GTH-GTHR binding mechanism and activation. In general, these receptors are
61 seen to show activity when the cognate stimulant/ligand binds to their biologically active binding

62 region called orthosteric binding site. Although the mammalian GTHR homologs in mammals
63 display high specificity to their cognate hormones, in case of fish, both FSHR and LHR exhibit
64 species-specific variability in ligand-binding promiscuity/specification, which complicates the use
65 of native ligands for receptor regulation. For example, in carp, FSHR is seen to be activated in
66 response to both cFSH and cLH⁹, whereas in tilapia, both GTHRs bind specifically to their cognate
67 receptors¹⁰. Simultaneously, in sturgeon¹¹ and medaka¹², both FSH and LH can activate each the
68 others cognate receptor in addition to their own. Despite being the center of GPCR-targeted drug
69 development, receptor modulation via orthosteric sites often lacks binding specificity, efficiency,
70 and efficacy. Moreover, due to the large size of GTHR orthosteric sites, small compounds are
71 unable to bind them and thereby change their conformation, impeding the use of low molecular
72 weight drugs for pharmacological regulation of these receptors.

73 As opposed to most class A GPCRs that possess an orthosteric binding domain in the
74 hydrophobic pocket created by the extracellular domain (ECD), the transmembrane domain
75 (TMD), the connecting extracellular loops (ECL), GTHRs belong to a subfamily of glycoprotein
76 receptors with an ECD that is nearly as large as the TMD. This domain contains a series of
77 leucine-rich repeat (LRR) domains that act as the orthosteric binding site, independently of the
78 TMD. Furthermore, the hinge region which connects the ECD to TMD acts as a intramolecular
79 modulator located between the ECD and TMD is thought to be essential for specificity in GTH-
80 GTHR interaction.¹³. Upon binding of the cognate hormone to the LRR region, this part moves to
81 interact with the hinge region, which then manipulates the TMD and ICD, leading to receptor
82 activation and downstream signal transduction^{7, 8}. Besides the orthosteric binding sites, several
83 allosteric binding sites have been localized on GPCRs. Allosteric sites may lie within orthosteric
84 binding pockets, overlap with them, or be topographically distinct. They can be located on the

85 ECD, inside and/or outside the TMD and on the extracellular loops (ECL) or intracellular loops
86 (ICL) of the receptor. Furthermore, these sites can accommodate agonistic, antagonistic, positive,
87 negative as well as silent modulators whilst enabling the manipulation of multiple signaling
88 cascades simultaneously. The allosteric sites on GTHRs are located in hydrophobic cavities
89 formed by the TMD and ECL (Fig. 1) and are not biologically active or accessible for the native
90 GTH, but can pose as common potential targets for small compounds that are highly effective
91 reproductive endocrine modulators. While Allosteric sites in most GPCRs often partially overlap
92 the orthosteric binding pocket in GTHR they are completely separated due to their unique ECD.

93 **Figure 1**



94 **A.)Glycoprotein hormone receptors**

B.)Other class-A GPCRs

95 **Figure. 1: Orthosteric and allosteric sites in glycoprotein receptors vs other class A GPCRs.**
96 Ribbon diagrams show a glycoprotein receptor (A.) where the orthosteric site is situated on a large
97 ECD that is separated from the TMD and does not overlap the allosteric site, as observed in other
98 class A GPCRs (B.).

99 A number of novel allosteric modulators have been reported for GTHRs over the past decade.
100 However, most of them target human FSHR (hFSHR) and may not be as efficient or effective on
101 GTHR homologs in other vertebrates like fish, which exhibit much more complex hormone-
102 receptor expression, interaction, and specificity. Based on their effect on signal transduction and
103 efficacy, the Allosteric modulators can be divided into four classes: agonists or antagonists that
104 can directly modulate receptor activity and induce signal transduction without the involvement of
105 additional ligands; positive (PAMs) and negative allosteric modulators (NAMs) that can potentiate
106 or reduce native ligand-mediated response and thereby play a supportive role; and neutral allosteric
107 ligands (NALs), which do not affect receptor activity after binding ¹⁴⁻¹⁷. A fifth category of
108 modulators (Biased Allosteric Modulators), which has recently emerged, is defined by the
109 signaling pathway-specific effects of the modulators on binding to designated receptors ¹⁸.
110 Thiazolidines, which were the first GTHR-specific allosteric modulators to be discovered, bind
111 exclusively to FSHR, showing no affinity to other glycoproteins such as LHR or thyrotropin
112 receptor ^{19, 20}. Nevertheless, some thiazolidine analogs may exhibit biased signaling and mobilize
113 either $G\alpha_s$, $G\alpha_i$ or both. Similarly, recent *in vivo* studies have identified TP22 ²¹ and Org43553 ²²
114 both of which are thieno[2,3-d]pyrimidine compounds as effective allosteric agonists of LHRs but
115 might potentially influence different signal cascades downstream.

116 To date, most published studies focus mainly on FSH modulators, with most reported
117 compounds being PAMs and NAMs. However, the screening process for allosteric modulators is
118 lengthy and costly, which calls for the necessity of novel *in-silico* tools to increase the hit rate of
119 the screening. However small compounds that modulate allosteric sites must overcome shallow

120 binding pockets, low binding affinity, desensitization or mutational resistance, dissatisfactory
121 ADME (absorption, distribution, metabolism, and excretion) values and the possibility of multiple
122 site affinity ²³. These limitations have called for the development of new tools to increase the hit
123 rate and efficiency of screening. With the development in the field of *in-silico* tools, the candidate
124 selection process and hit rates for these compounds have improved significantly. In this study, we
125 have generated site-specific pharmacophore hypothesis based on the allosteric cavity at the site of
126 interest. Combined with multiple *in-silico* screening methods, this approach enabled us to identify
127 effective small compounds with high potential to act as agonists for carp GTHRs. Our *in vitro*
128 results have confirmed that these compounds are independent modulators of GTHRs with high
129 receptor specificity.

130 Materials and Methods

131 Homology modeling

132 3D homology models for carp cFSHR and cLHR were generated using hLHCGR homologs
133 (PDB: 7FIG; 7FIH; 7FII; 7FIJ) as a template for both inactive and active states using the I-
134 TASSER server *in silico* (Zhang 2009; Roy et al. 2012). The top models were selected based on
135 C-score, structural stability, and structural similarity with the gonadotropin receptors. The protein
136 models were further rendered and prepared using Maestro tool in Schrodinger software (Maestro,
137 Schrödinger, LLC, New York, NY, 2021.).

138 Pharmacophore model hypothesis, ligand screening and docking.

139 Potential binding sites in the cFSHR and cLHR TMDs were detected using SiteMap module
140 (Schrödinger, LLC, New York, NY, 2021) and selected based on their position in the TMD cavity.
141 We then used these data to generate receptor cavity-based pharmacophore hypothesis. GPCR

142 library (version 24 May 2020; <https://enamine.net/compound-libraries/targeted-libraries/gpcr-library>) (~54000 compounds)) and allosteric GPCR library (version 28 February 2019; 143 <https://enamine.net/compound-libraries/targeted-libraries/gpcr-library/allosteric-gpcr-library>) 144 (~14400 compounds) were downloaded from Enamine website (Enamine Ltd). The compound 145 libraries were converted to phase databases and then screened using the Phase module of 146 Schrodinger software, based on the generated receptor cavity-based and ligand-based hypothesis 147 ²⁴. The ECD domain, excluding most of the hinge region, was cleaved off, and ligands were docked 148 only onto the transmembrane allosteric binding pocket on carp GTHR using GLIDE module of 149 Schrodinger software ²⁵. To further screen the candidates, we used QikProp (Schrödinger, LLC, 150 New York, NY, 2021) to predict ADME properties. Docked ligands were then further screened 151 using g-score, docking score and e-model score, resulting in the selection of 20 small compounds 152 for both cFSHR and cLHR. Four small compounds were eventually selected for *in vitro* studies 153 based on predicted structural alignment to the receptor cavity. The interactions between the 154 selected ligands and receptors were then analyzed *in silico* and compared to activation by 155 orthosteric ligands. 156

157 LUC Transactivation assay

158 Transient transfection, cell procedures and stimulations were generally performed as described 159 previously ^{10, 26, 27}. Briefly, COS-7 cells were grown in DMEM supplemented with 10% FBS, 1% 160 glutamine, 100 U/ml penicillin, and 100 mg/ml streptomycin (Biological Industries, Israel) under 161 5% CO₂ until confluent. The selected compounds (Z2242908028 (here on “8028”), 162 Z1456504681(here on “4681”), Z2242909045(here on “9045”), Z1456630801(here on “0801”)) 163 (Supplementary Spreadsheet. 1) were purchased from Enamine (Enamine Ltd., Kyiv, Ukraine). 164 Co-transfection of the receptors (at 3 µg/plate) and cAMP response element-luciferase (CRE-Luc)

165 reporter plasmid delivery (3 μ g/plate for cFSHr and 0.3 μ g/plate for cLHr) was carried out with
166 TransIT-X2® System (Mirus). The cells were serum-starved for 16 h, stimulated with the various
167 stimulants (initial concentration of 2 μ g/ml diluted continually 1:3) for 6 h, and then harvested and
168 analyzed. Recombinant carp LH (Aizen et al., 2012) and FSH (Hollander-Cohen et al., 2018) were
169 used as positive controls. Lysates prepared from the harvested cells were assayed for luciferase
170 activity, as described previously ²⁷. Experiments were repeated at least three times from
171 independent transfections, and each was performed in triplicate. Non- transfected COS& cells
172 were used as negative control to ascertain the activity of the ligands is receptor specific.

173 **Statistical analysis**

174 EC₅₀ values were calculated from concentration-response curves by means of computerized
175 nonlinear curve fitting (log(agonist) vs. response (three parameter)) using GraphPad PRISM 9
176 (version 9.5.0). The potency ratio was calculated as the Log(Relative Potency)= Log(EC50 of the
177 native compound) – Log(EC50 of the novel compound) ²⁸.

178 **Results & Discussion**

179 To generate homology models for carp FSHR and LHR we used available crystal structures of
180 human homologs (PDB ID: 7FIH & 8I2H, for cLHR and cFSHR, respectively) ^{7 29}, as the carp
181 homologs displayed high similarity and features characteristic of human GTHRs. These
182 glycoprotein receptors belong to the class-A rhodopsin-like family of GPCRs ³⁰, whose structure
183 is generally divided into three parts (Fig. 1): an N-terminal extracellular domain (ECD), seven
184 interconnected serpentine transmembrane helices (1-7 TMD) and an intracellular domain (ICD)
185 containing the C terminus ³¹.

186 Comparison between the sequences of human and carp receptors revealed high similarities
187 (Table 1). Though the percentage of structural similarities between the whole mammalian
188 receptors to the fish receptors was relatively high, ranging from 61% to 67%, the TMD appeared
189 to be much more conserved (75% - 82% similarities), suggesting conserved activation mechanism
190 and function for this domain. Moreover, while cFSHR TMD is more similar to hFSH TMD than
191 to that of hLHR, cLHR TMD is equally similar to both human receptors (Table 1).

192 **Table 1.** Sequence similarity between carp and human GTHRs

Receptors	cLHR		cFSHR	
	Whole	TMD	Whole	TMD
hLHR	66%	75%	61%	75%
hFSHR	64%	75%	67%	82%
cLHR	100%	100%	60%	74%

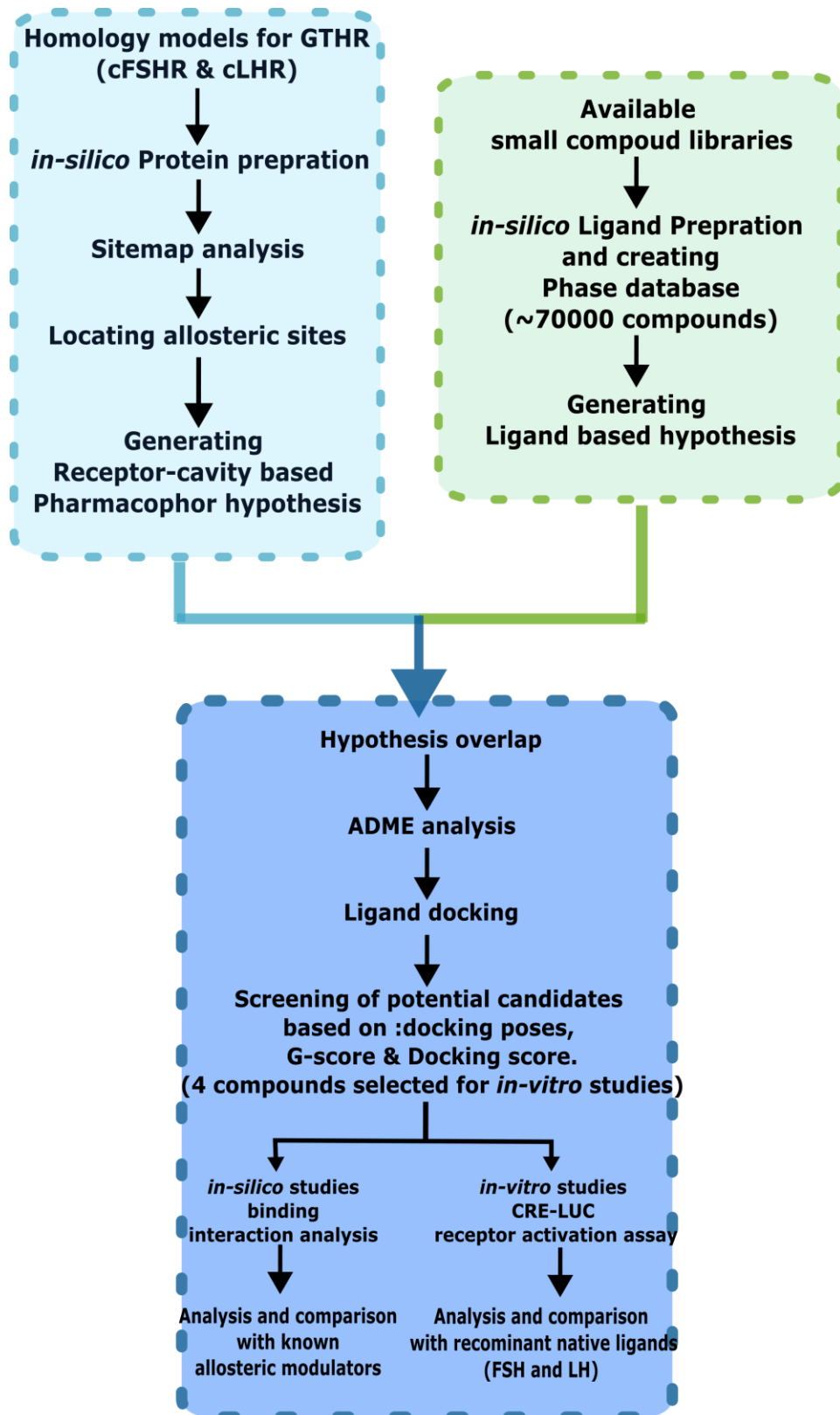
193 **Table 1.** “Whole” was defined as the entire receptor including ECD, TMD extra- and
194 intracellular loops and ICD, whereas “TMD” includes the extra- and intracellular loops that
195 connect the helices.

196 Traditionally, orthosteric binding sites have been considered the preferred targets for drug
197 development. However, targeting these sites can lead to activation of multiple signaling cascades.
198 For example, the human GTHR can activate internal signal proteins such as Gq/11, Gi/0, IP3, and
199 β -arrestin to regulate various intracellular pathways and mediate receptor internalization, in
200 addition to G proteins and adenylate cyclase pathways. This complexity limits the ability to
201 precisely control synthetic modulation of the receptor³². Despite consistent progress in developing
202 GPCR-targeting allosteric modulators, the enormity of receptor and hormone renders the
203 manipulation of these receptors much more complicated. Hence, only a few small compounds are
204 available for its modulation. We therefore strived to search for candidates that exhibit the potential
205 to directly modulate these receptors. For which, we analyzed *in-silico* the generated structures for

206 possible binding sites and located orthosteric sites on the ECD and allosteric binding sites within
207 the TMD of cGTHRs (Fig. 2; Fig. S1) ^{7,29}.

208 As the allosteric sites are located close to the ECLs, we hypothesized that the small compounds
209 binding to this site would induce conformational changes similar to those caused by orthosteric
210 binding mechanism. Studies in humans have demonstrated potent allosteric modulation of hFSHR
211 by small compounds, such as Cpd-21f and Org214444-0. These compounds are 10 to 100 times
212 more potent in activating hLHR than in activating hFSHR. The binding site of Cpd-21f and Org-
213 214444-0 almost completely overlapped with that of ligand Org43553 on luteinizing
214 hormone/choriogonadotropin receptor (LHCGR) ^{7,8}. When binding to its allosteric destination on
215 LHCGR receptor, Org43553 was reported to be an almost full agonist, inducing a selective
216 agonistic effect and showing signal cascade specificity ³³. The allosteric binding pockets in hFSHR
217 and hLHCGR are very similar, and both are mainly composed of residues on TM3, TM5, TM6
218 and TM7, along with ECL2 and ELC3. The recently published electron microscopy structure of
219 human LHCGR shows Org43553 binding deep in the allosteric pocket at the top half of the TMD
220 (PDB:7FIH), mainly via hydrophobic interactions. Org43553 was reported to be exposed to the
221 hinge domain and ECL ⁷, which induces conformational modulation of the receptor. Based on
222 these findings, we generated a receptor cavity-based pharmacophore hypothesis which is a
223 pharmacophore hypothesis based on the nature of residues on the receptor that are exposed to
224 allosteric binding pockets in the TMD of both cFSHR and cLHR (Fig. 3).

225 **Figure 2**



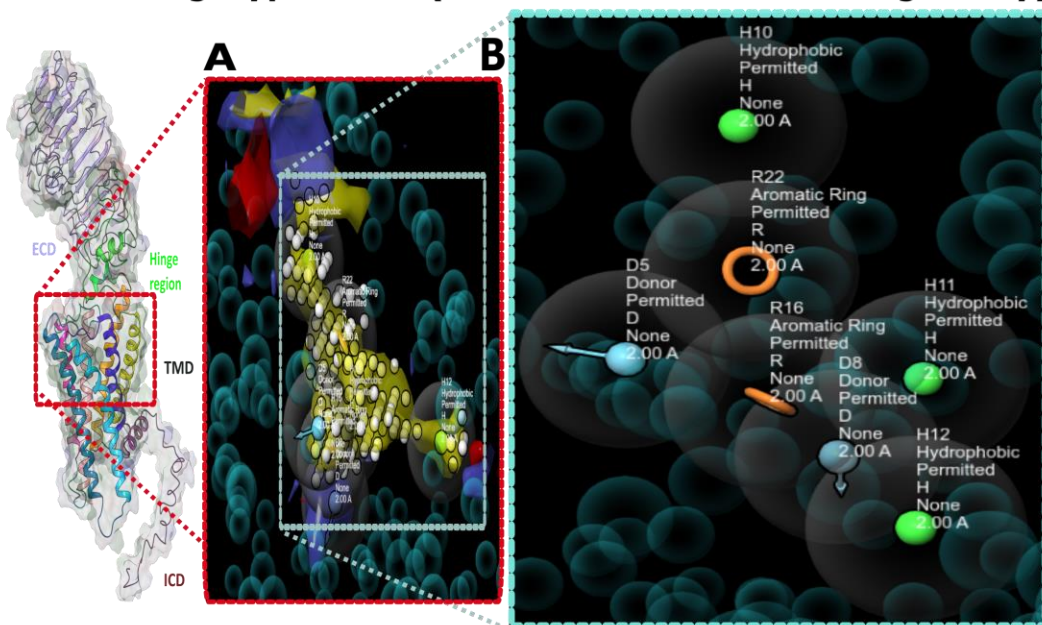
226

227 **Figure 2:** Receptor cavity-based screening procedure for selected compounds.

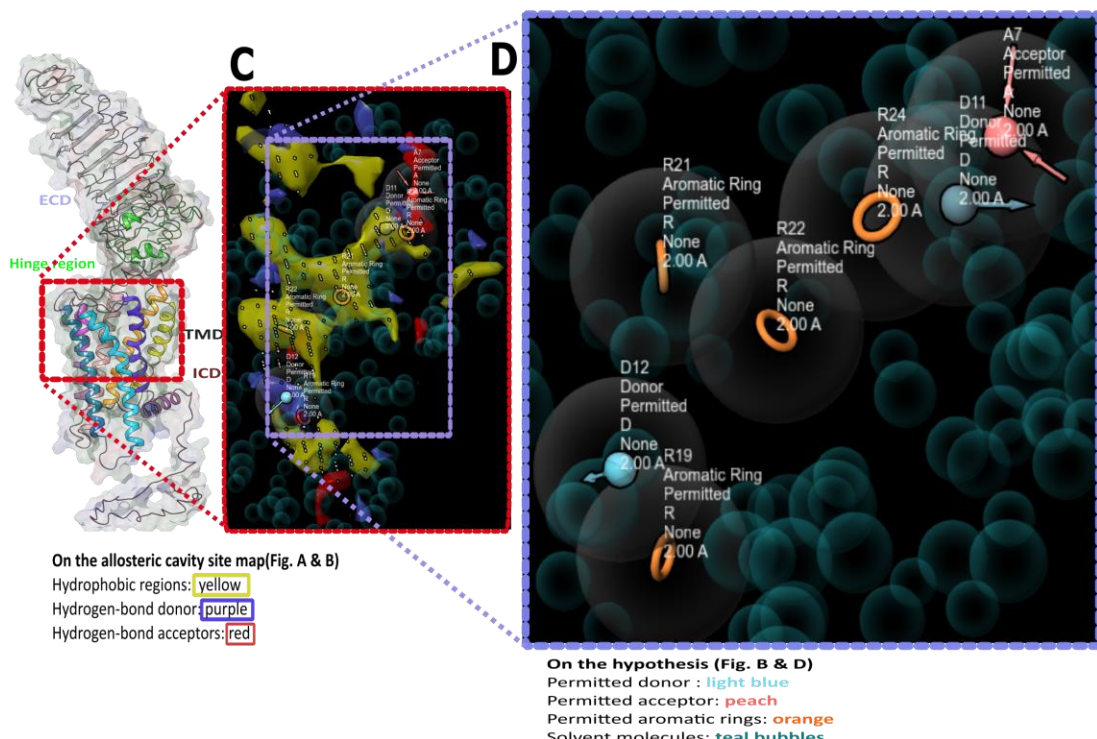
228 GPCR library (54080 compounds <https://enamine.net/compound-libraries/targeted-libraries/gpcr-library>) and allosteric GPCR library (14400 compounds
229 <https://enamine.net/compound-libraries/targeted-libraries/gpcr-library/allosteric-gpcr-library>)
230 were retrieved from Enamine website and were converted to Phase format (see Experimental
231 procedures). We then screened the ligand database based on the generated hypothesis and
232 performed an ADME analysis. We generated ligand-based hypothesis and used them in parallel
233 with the receptor cavity-based hypothesis as an additional screening step and docked the chosen
234 ligands onto the allosteric site. The most successfully docked small compounds were shortlisted
235 based on Glide g-score, XP g-score and Docking score. The docking conformation was selected
236 on the basis of Glide emodel.
237

238 **Figure 3**

cFSHR-drug Hypothesis (based on allosteric binding cavity)



cLHR-drug Hypothesis (based on allosteric binding cavity)



239

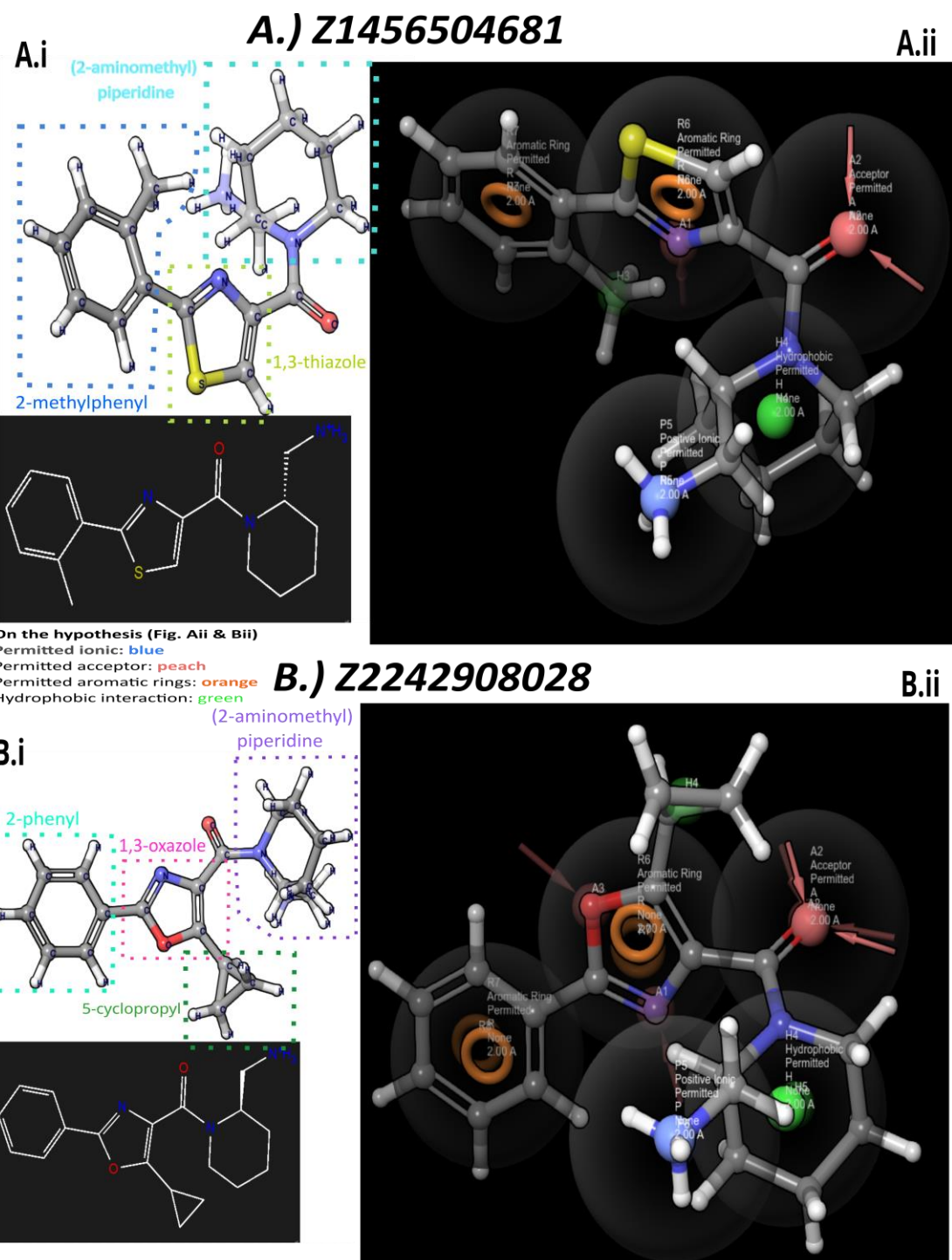
240 **Figure. 3: Receptor cavity-based hypothesis map for allosteric modulation.** Models showing
241 the surface of exposed residues in the allosteric binding pockets of cFSHR (A) and cLHR (C) and
242 the corresponding receptor cavity-based hypothesis (B, D). Small compounds were screened using
243 these hypotheses to select suitable candidate modulators.

244 Eventually, two compounds were selected for each receptor and tested *in vitro*. These included
245 8028 [1-(5-cyclopropyl-2-phenyl-1,3-oxazole-4-carbonyl)piperidin-2-yl]methanamine; 4681 (1-
246 [2-(2-methylphenyl)-1,3-thiazole-4-carbonyl]piperidin-2-yl)methanamine hydrochloride ; 9045
247 (1-(2-[(2-chlorophenyl) methoxy] benzoyl) pyrrolidin-3-yl) methanamine; and 0801 (1-[5-(2,3-
248 dihydro-1,4-benzodioxin-6-yl) -1,3-oxazole-4-carbonyl] pyrrolidin-3-yl) methanamine
249 dihydrochloride) (Figs. 4 and 5).

250 The effect of the selected compounds was tested using a receptor transactivation assay on
251 mammalian COS7 cells with cFSHR and cLHR co-transfected together with cAMP response
252 element-luciferase (CRE-LUC), which had been previously shown to be the dominant signal for
253 gonadotropin receptors ⁹. The activity of each compound, as determined by maximum response
254 and EC₅₀), was compared to the activity of the recombinant protein previously shown to activate
255 each receptor ^{9,10}. All the four molecules induced agonistic activation of the receptors, albeit with
256 varying response levels and efficiencies toward the different receptor types. The cFSHR was
257 activated by molecules 0801 and 8028 (maximum response, 1.406 and 1.499; EC₅₀, 23.8 and 4.134
258 nM, respectively) more efficiently than the recombinant ligands cFSH and cLH at significantly
259 lower EC₅₀ values (maximum response, 1.506 and 1.425; EC₅₀, 146.5 and 172.8 nM, respectively)
260 (Table 2; Figs. 6 and 7). There was no significant response seen in non GTHR transfected cell lines
261 in response to the selected ligands.

262

263 **Figure 4**

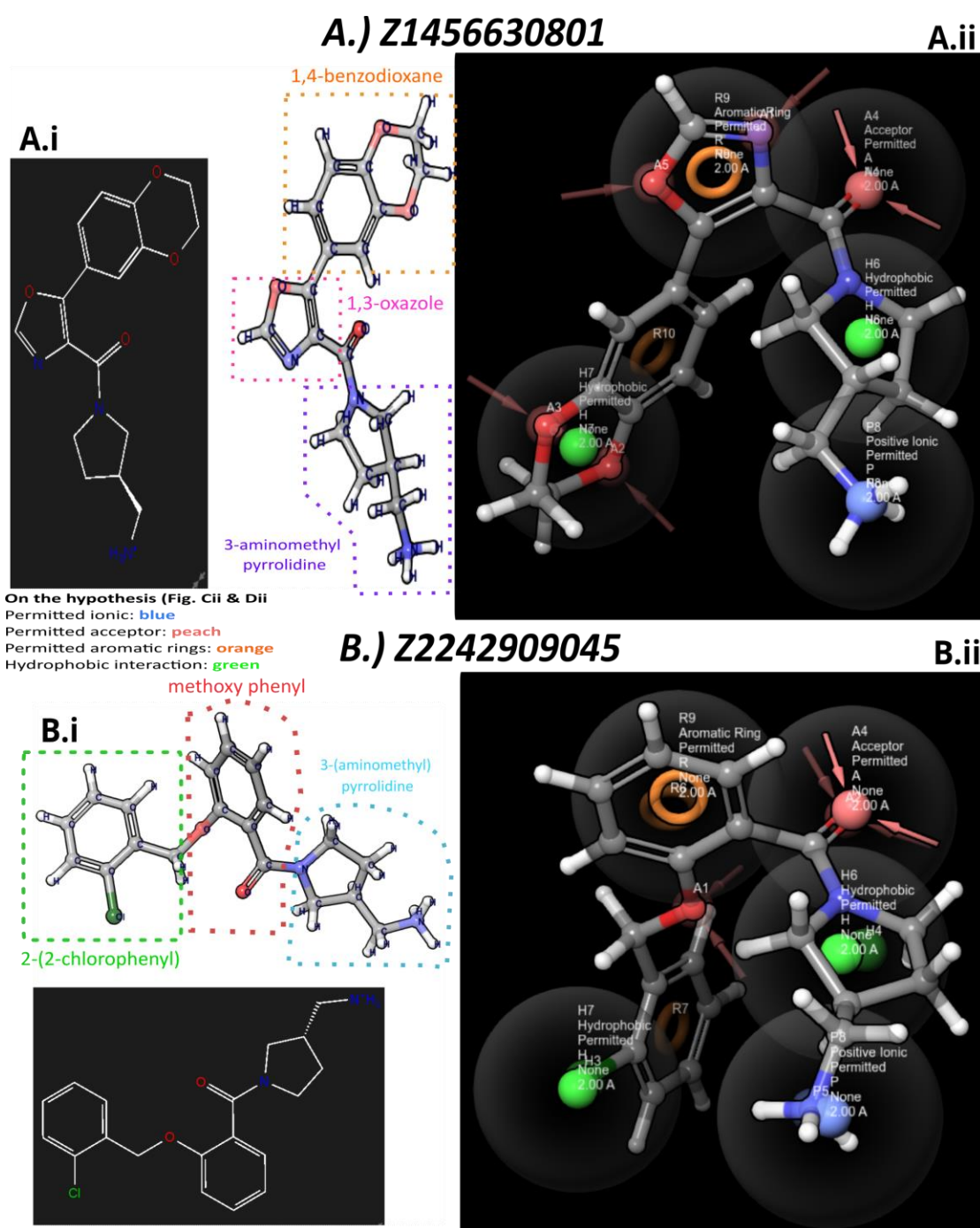


A.) Z1456504681:{1-[2-(2-methylphenyl)-1,3-thiazole-4-carbonyl]piperidin-2-yl}methanamine hydrochloride
 B.) Z2242908028:[1-(5-cyclopropyl-2-phenyl-1,3-oxazole-4-carbonyl)piperidin-2-yl]methanamine

264
 265 **Figure. 4: Pharmacophore overlap with the screened ligands Z1456504681 and**
 266 **Z2242908028.**
 267 **Ai;Bi:** 3D and Kekulé structures of the tested compounds.
 268 **Aii,Bii:** Overlap of receptor cavity and ligand based Hypothesis on the small compounds.

269

Figure 5



A.) Z1456630801: {1-[5-(2,3-dihydro-1,4-benzodioxin-6-yl)-1,3-oxazole-4-carbonyl]pyrrolidin-3-yl}methanamine dihydrochloride
 B.) Z22242909045: (1-{2-[(2-chlorophenyl)methoxy]benzoyl}pyrrolidin-3-yl)methanamine dihydrochloride

270

Figure. 5: Ligand hypothesis overlap.

271 **Ai;Bi:** 3D and Kekulé structures of the tested compounds.
 272 **Aii,Bii:** Overlap of receptor cavity and ligand based HypothesisHypothesis overlap on the small
 273 compounds.
 274

275 cLHR was activated by molecules 8028 and 4681 (max response, 1.210 and 1.164; EC₅₀, 610.5
276 and 300.6 nM, respectively) at similar levels as the recombinant cLH (max response, 1.216; EC₅₀,
277 303.3 nM) (Table 2). Therefore, we report molecules 4681 and 0801 as specific agonists of cLHR
278 and cFSHR, respectively. Moreover the 4681 appear to be potential antagonist for FSHR and 0801
279 for cLHR. Molecule 8028 is a dual agonist for both receptors; however, it activated cFSHR at a
280 significantly lower dose. Regarding molecule 9045, although it also activated both receptors, the
281 EC₅₀ values reflect a very low efficiency compared to the recombinant ligands. Despite both 4681
282 and 0801 showing potential antagonistic behaviour towards the cFSHR maximal response at some
283 doses spiked, this might be the result of constitutive activity of the receptor that remain unblocked
284 by the antagonist. (Table 2).

285 **Table 2.** EC50 values and activation potency of the tested small compound vs the native ligands.

286

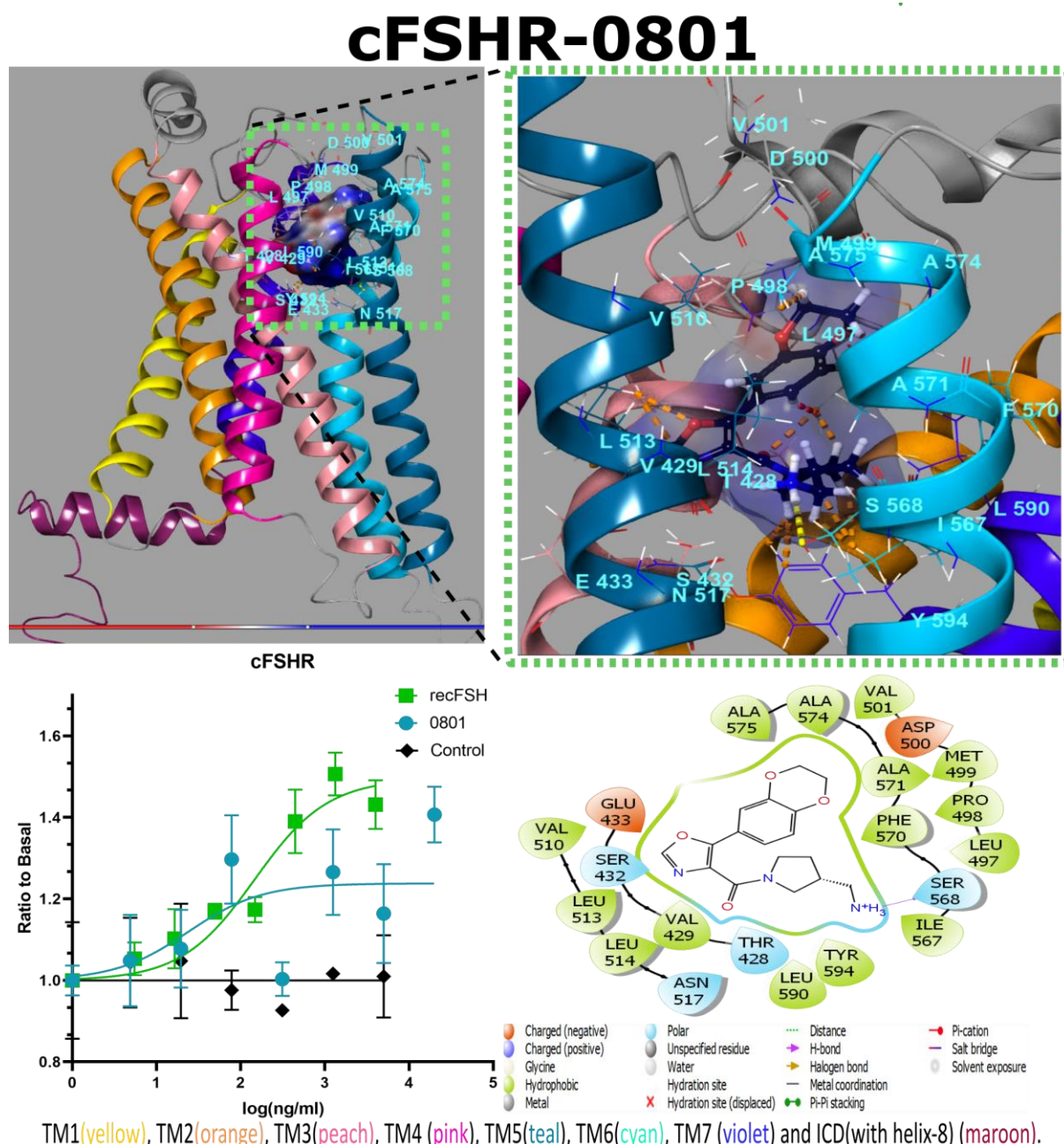
Ligands	M.W (kDa)	Receptors										Ligand performance	
		cFSHR						cLHR					
		EC ₅₀ (nM)	EC ₅₀ (ng/ml)	log EC ₅₀ (ng/ml)	Max. Response	log (Relative Potency)		EC ₅₀ (nM)	EC ₅₀ (ng/ml)	log EC ₅₀ (ng/ml)	Max. Response	log (Relative Potency)	
recF SH	25	5.86	146.5	2.166	1.50655	0	0	-	-	-	-	-	cFSHR specific native hormone
recL H	30	5.76	172.8	2.482	1.42585	-0.316	10.11	303.3	0	1.21619	0	0	cFSHR & cLHR native hormone
9045	0.344835	9882.988	3408	3.532	1.30924	-1.366	26937.52	9289	-1.485	1.39297	-1.485	0	High agonist for cFSHR & cLHR
0801 *	0.32935	72.26355	23.80	1.377	1.40680	0.789	16.49917	5.434	1.7468	1.03843	1.7468	0	cFSHR specific agonist and potential antagonist for cLHR
8028	0.325405	12.70417	4.134	0.6164	1.49917	1.5496	1876.124	610.5	-0.304	1.21069	-0.304	0	cFSHR & cLHR selective agonist (partial towards cFSHR)
4681 *			30.84	1.489	1.22959	0.677	300.6		0.004	1.16487	0.966406	0	cLHR specific agonist and potential antagonist for cFSHR
0.315433	97.77037												

287 **Table 2:** Relative Potency was defined as log (Relative Potency) = log (EC₅₀ of the native
288 compound) – log (EC₅₀ of the novel compound).

289 *Compounds 0801 and 4681 showed potential antagonistic behavior towards cLHR and cFSHR
290 respectively and are marked in red as the ratio does not reflect the overall performance of these
291 small compound.**No significant activity was found by non-transfected Cos7 cells on simulation
292 with the ligands.

293

294 **Figure 6**



295

296 **Fig. 6: Interactions between cFSHR and Z1456630801.** The molecule has 1,3-oxazole in its
297 core, like Z2242908028, instead of dihydroimidazole core on Cpd-21f. This oxazole is attached to
298 1,4-benzodioxane and 3-aminomethyl pyrrolidine functional groups. On the latter, the
299 aminomethyl sidechain interacts with I567^{6.51} and S568^{6.52} on the TM6 of the receptor via hydrogen
300 bond, whereas L513^{5.43} (TM5) and Y594^{7.42} (TM7) are involved in hydrophobic interactions.
301 Simultaneously, the oxazole interacts with E433^{3.37} (TM3) and L513^{5.43} (TM5). The graph shows
302 CRE-luciferase activity in response to the tested molecule and recombinant carp FSH as a function
303 of concentration. The control denotes to activity of the non-transfected COS 7 cell in response
304 towards concerned ligand.

305 The 0801, which specifically activated cFSHR, bound to an allosteric binding site that is
306 positioned similarly to the binding sites reported for Cpd_21f-cLHR and Org43553-cFSHR
307 interactions in human homolog ^{7,8}; however, it interacted with the lower region of the binding
308 pocket, majorly via hydrophobic interactions (Figs. 4ii and 6). The 1,4-benzodioxane group is
309 exposed to the cFSHR ECL2 and interacts with M499_{cFSHR}, but simultaneously it also showed
310 interactions with A571^{6.55}_{cFSHR} and A575^{6.59}_{cFSHR}. *In silico* analysis showed that various
311 substitution mutations in I567^{6.51}_{cFSHR} and A571^{6.55}_{cFSHR} on TM6 caused the most significant
312 decrease in complex stability and ligand affinity; thus, these residues may play a key role in
313 receptor activation. Mutations in similarly positioned homologs in hLHCGR (I585^{6.51}W_{hLHCGR} and
314 A589^{6.55}F_{hLHCGR}) have been reported to reduce the ability of Org43553 to activate the receptor.
315 cLHR was not activated in response to 0801 (Fig. S2) and its activity even slightly decreased with
316 increasing doses, suggesting this molecule as a potential NAM/NAL for cLHR.

317 The compound 8028, which was more partial towards cFSHR, has an oxazole at its core attached
318 to piperidine, phenyl and cyclopropyl sidechains (Fig. 4Bi, Bii). The phenyl ring interacts with
319 ECL2, which functions as an intramolecular modulator of the TMD.

320 In vitro results along with structural interactions suggests that the interaction between M499_{cFSHR}
321 and V501_{cFSHR} on the ECL2 of cFSHR is crucial for receptor activation, as these interactions were
322 observed in the 8028 binding but not in 4681 (Fig. S3), which did not activate the receptor. The
323 activation of cLHR in response to 8028 was similar to the response to its native ligand cLH. Our

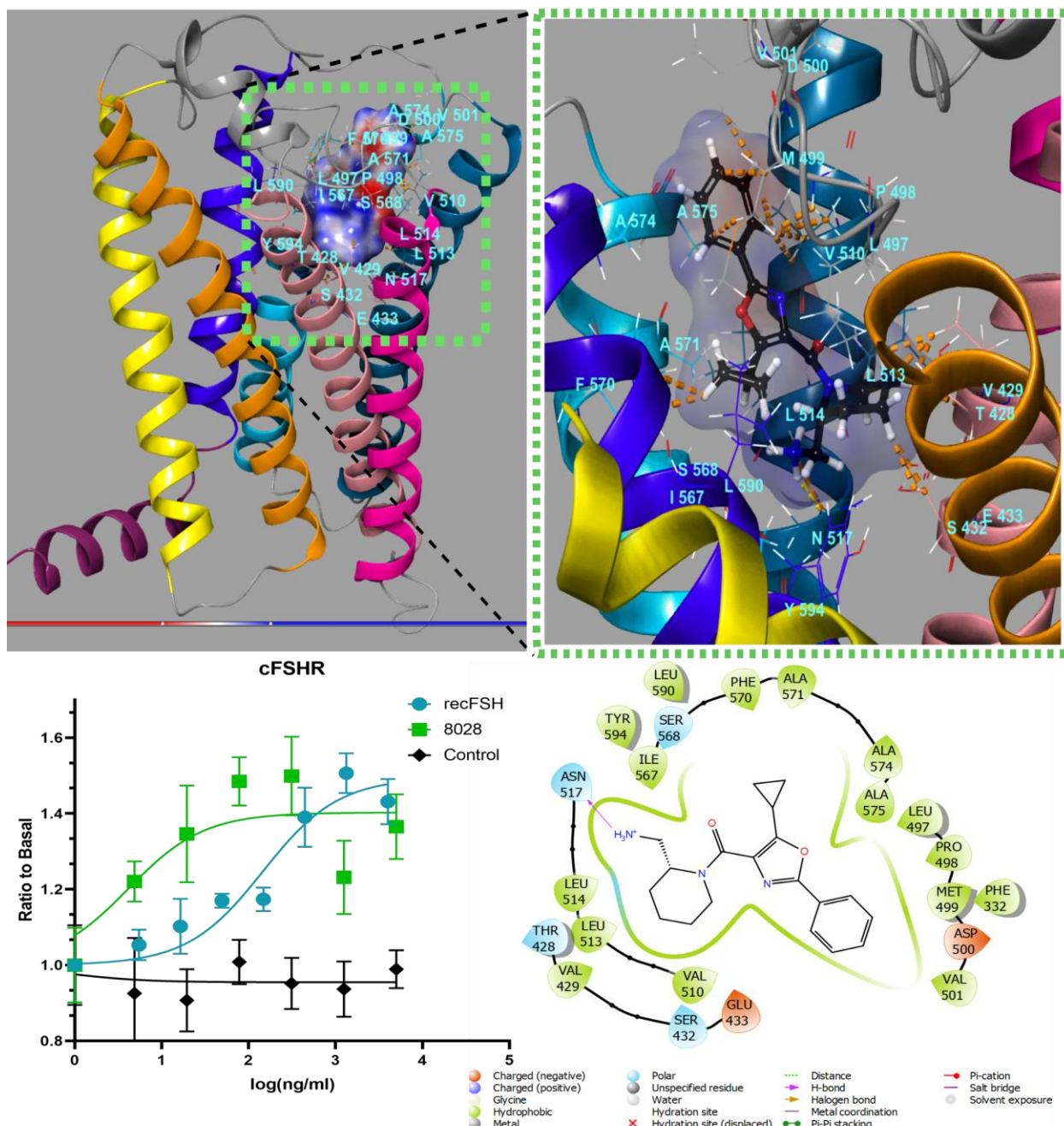
324 studies show that docking of 8028 to cLHR occurred comparatively deeper within the allosteric
325 binding cavity of the receptor (Figs. 5i and 7). The phenyl ring attached to the oxazole is also
326 exposed to ECL2 and interacts particularly with M534_{cLHR}, P533_{cLHR}-, which are positioned
327 similarly to M499_{cFSHR} and V501_{cFSHR} on cFSHR. *In silico* mutation analysis showed that
328 substituting homologous cLHR residues L532_{cLHR}, P533_{cLHR} and M534_{cLHR} with various amino
329 acids considerably reduced binding stability and affinity. Despite the conformational variance, the
330 interacting amino acids on cFSHR and cLHR are significantly conserved.

331 The ECL2 is the largest intracellular loop of both cFSHR and cLHR. Studies in hFSHR have
332 established that ECL2 is indispensable in mediating post-docking conformational changes by
333 interacting with other ECLs and TMDs. The homologous mutation P519T_{hFSHR}(P533_{cLHR}), which
334 is positioned on hFSHR-ECL2, has been associated with primary amenorrhea in patients, whereas
335 V514A_{hFSHR} (V501_{cFSHR}) mutation was observed in patients undergoing *in vitro* fertilization who
336 exhibited symptoms of iatrogenic ovarian hyperstimulation syndrome. Further, the P519T
337 mutation on hFSHR ECL2 ultimately impaired adenylate cyclase stimulation *in vitro* ^{34, 35}.
338 P519_{hFSHR} is highly conserved in hFSHR(P516_{hLHCGR}), cFSHR(P498_{cFSHR}) and cLHR(P533_{cLHR}),
339 and its mutation was reported to disrupt receptor trafficking to the cell surface and subsequently
340 abolished FSH binding and cAMP production ²⁹. Therefore, the interaction of the ligand with this
341 residue might explain its agonistic effect on cLHR and cFSHR. Further, whereas F515^{ECL2}A_{hLHCGR}
342 (homologs L532^{ECL2}_{cLHR}, L497^{ECL2}_{cFSHR} and L518^{ECL2}_{hFSHR}) and T521^{ECL2}A_{hLHCGR} (homologs
343 L538^{ECL2}_{cLHR}, L503^{ECL2}_{cFSHR} and L524^{ECL2}_{hFSHR}) mutations on hLHR ECL2 enhanced
344 internalization and cAMP signaling, S512A_{hLHR} (S529_{cLHR}, F515_{hFSHR},) and
345 V519A_{hLHR}(homologs I536^{ECL2}_{cLHR}, V501^{ECL2}_{cFSHR} and I522^{ECL2}_{hFSHR}) impaired these processes
346 ³⁶. This indicates that ECL2 might play a key role in selective activation of downstream signal

347 transduction and impact its efficiency significantly and is therefore a potential target for signaling
348 pathway-specific selective modulators.

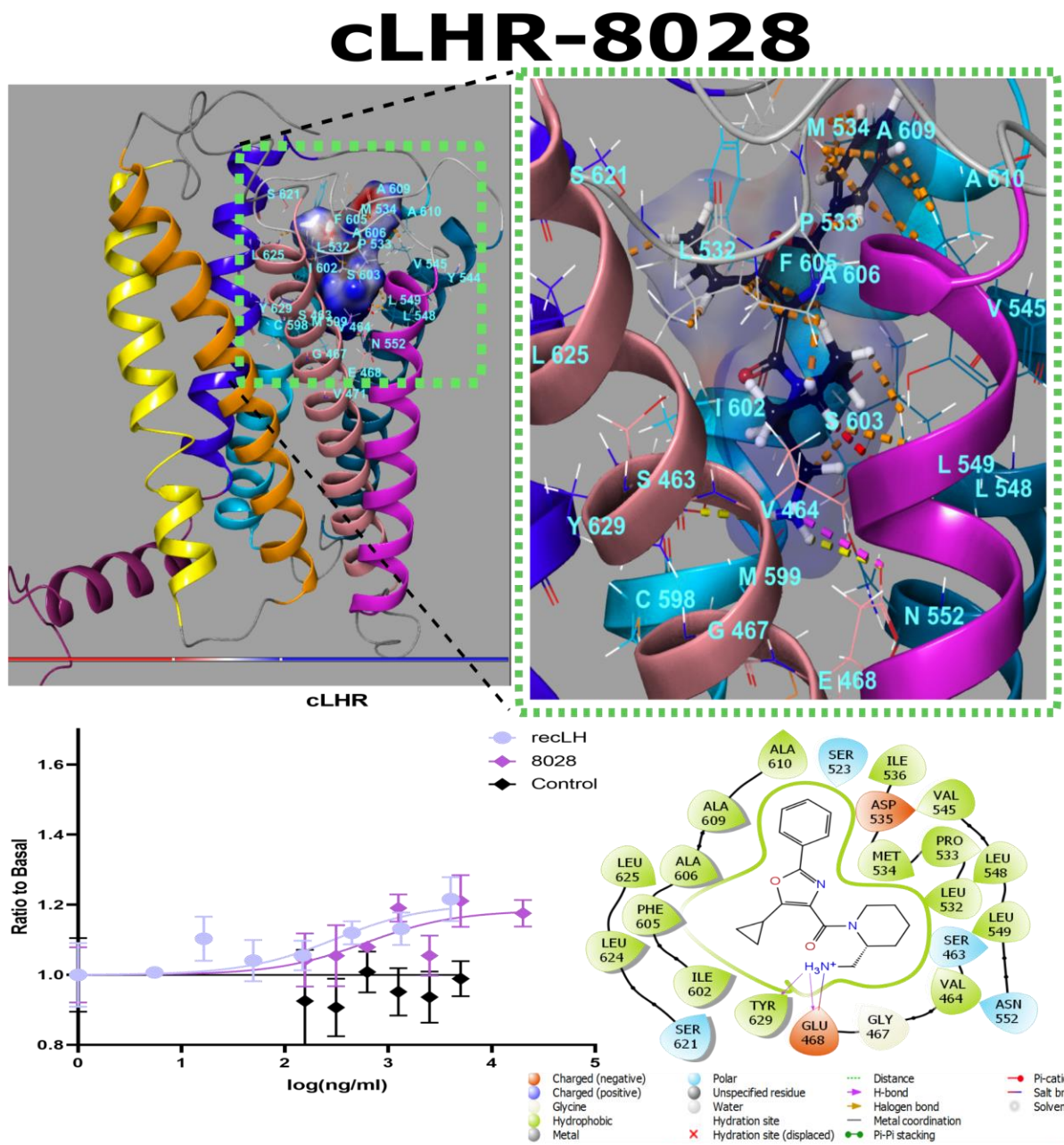
349 **Figure 7**

cFSHR-8028



350 TM1(yellow), TM2(orange), TM3(peach), TM4(pink), TM5(teal), TM6(cyan), TM7(violet) and ICD(with helix-8) (maroon).

351 **Fig. 7. Interactions between cFSHR and Z2242908028.** The molecule's oxazole core is attached
352 to piperidine, phenyl and cyclopropyl sidechains. The phenyl ring was observed to associate with
353 M499 and V501 on ECL2 and with V510^{5,40} on TM5. The cyclopropyl interacts with F570^{6,54}
354 (TM6), whereas 2-aminmethyl piperidine interacts with V429^{3,33} (TM3), S432^{3,36} (TM3), L513^{5,43}
355 (TM5) and N517^{5,17} (TM5). The graph shows CRE-luciferase activity in response to the tested
356 molecule and recombinant carp FSH as a function of concentration. The control denotes to activity
357 of the non-transfected COS 7 cell in response towards concerned ligand.



359 **Fig. 8: Interactions between cFSHR and Z2242908028.** This compound docked comparitively
360 deeper into the allosteric cavity. Both the 1,3-oxazole core and the attached 5-cyclopropyl and (2-

361 aminomethyl) piperidine sidechain closely interacted with L532 on ECL2, whereas the phenyl ring
362 interacted with M534 and P533 on ECL2. Major interactions were observed with hydrophobic
363 residues on TM5 (V545^{5,40}, L548^{5,43} and L549^{5,44}) TM6 (A606^{6,55} and A609^{6,58}) and TM7
364 (L625^{7,38}). The graph shows CRE-luciferase activity in response to the tested molecule and
365 recombinant carp LH as a function of concentration. The control denotes to activity of the non-
366 transfected COS 7 cell in response towards concerned ligand.

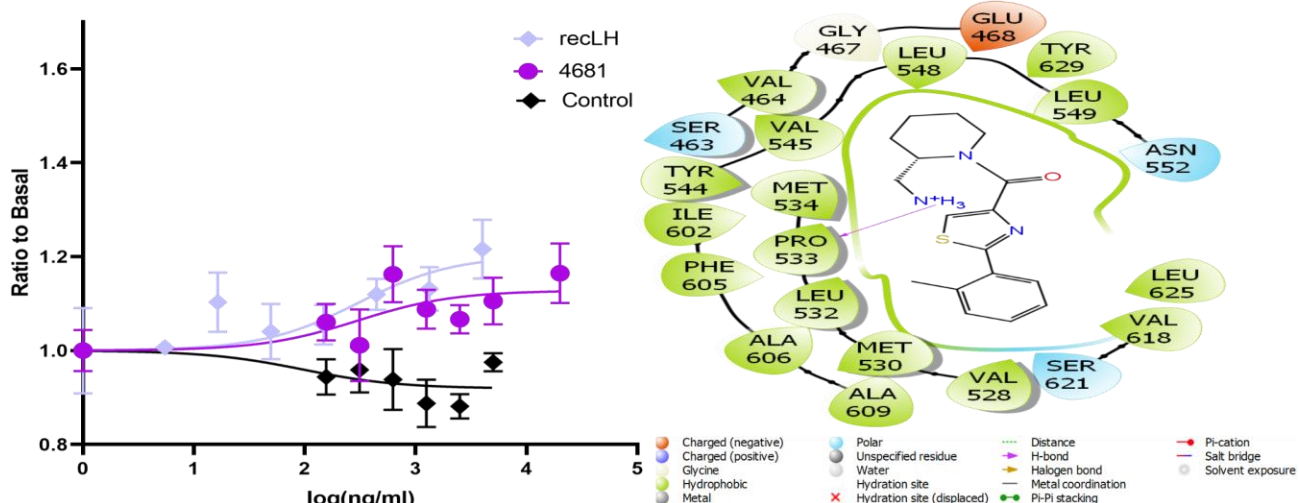
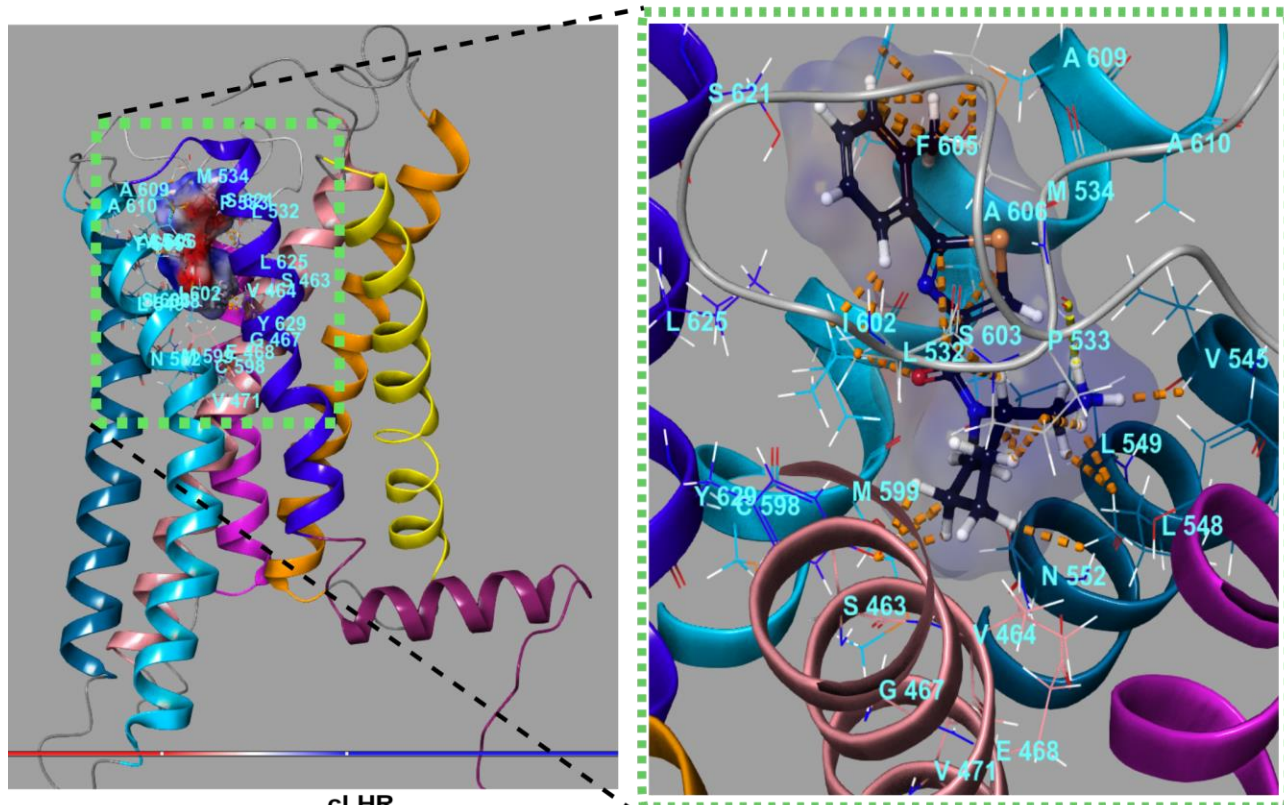
367 The cLHR ELC2 showed interactions with the hinge domain and ECL1, and *in silico*, mutations
368 in L532A_{cLHR}, P533A_{cLHR}, M534A_{cLHR} on ECL2 were seen to substantially reduce complex
369 stability and ligand affinity (Fig. 8). The oxazole was also observed to interact with A606^{6,55}_{cLHR}
370 on TM6, which seems to play a crucial role in 8028 binding. *In silico* mutations analysis showed
371 that substitution of cLHR A606^{6,55} with various amino acids (A606F_{cLHR}, A606D_{cLHR}, A606R_{cLHR},
372 A606W_{cLHR}) caused the most significant decrease in complex stability and ligand affinity. Studies
373 have shown that mutation in the similarly positioned hLHCGR residue A589^{6,55}W_{hLHCGR} has
374 reduced activation by Org43553⁷, suggesting its role in allosteric receptor activation. As 8028
375 docking occurs comparatively deeper inside the allosteric TMD binding pocket of cLHR, it shows
376 many more interactions with the TM helices than when docking onto cFSHR. We hypothesize that
377 these interactions might hamper the post-binding conformational changes, therein reducing the
378 activation of cLHR by 8028 compared to cFSHR.

379 The compound 4681 induced a similar response in cLHR activity as did 8028, which also has a
380 similar structure. However, the oxazole core of 8028 is replaced by 1,3-thiazole in 4681, and the
381 cyclopropyl side chain is absent (Fig. 4i). Another difference is the presence of a 2-methylphenyl
382 group attached to the thiazole core, instead of a phenyl ring. This bulkier functional group leans
383 more backward towards the TM7, while the methyl extension interacts with F605^{6,54} on cLHR
384 TM6. At the opposite end, the phenyl ring simultaneously associates with L532 on ELC2, which
385 might slightly restrict TM6 movement (Fig. 9), whereas the shorter phenyl group of 8028 binds to
386 A609^{6,58}_{cLHR} and M534^{ELC2} instead. Although the cyclopropyl sidechain lacks interactions with

387 the 2-aminomethyl piperidine group, Y629 seems to compensate for the lack of interaction with
388 L625^{7.38} positioned on TM7, which appears to play a crucial role in the conformational modulation
389 of TM7. Moreover, (2-aminomethyl) piperidine interacts with Y629, which is situated
390 comparatively much deeper and hence might impair TM7 movement, further reducing the
391 activation potential of 4681. This might explain the lower potency values observed in response to
392 this molecule (Table 2). Although 4681 bound to cFSHR, the observed receptor activity was
393 significantly lower than cFSH. The residue mostly interacted with the deep hydrophobic pocket
394 created by the TM helices and showed no contact with the ECL2, which we hypothesize is crucial
395 for allosteric site-mediated docking and signal pathway specificity. The cFSHR, being
396 promiscuous, is activated not only by its cognate ligand cFSHR, but also by cLHR⁹. The compound
397 showed strong interactions with M499_{cFSHR}, L513^{5.43}_{cFSHR}, I567^{6.51}_{cFSHR} and A571^{6.55}_{cFSHR}, which
398 seem crucial for cFSHR activation. With its considerably low receptor activation, 4681 has
399 substantial potential as a cFSHR NAL/NAM or a cLHR-specific allosteric agonist.

400 The 9045 induced receptor activation at much higher concentrations than both 8028 and recFSH,
401 but a gradual dose-dependent increase was observed. Its docking conformation notably differed
402 between binding to cFSHR and cLHR. The molecule has a methoxyphenyl core that is attached to
403 2-(2-chlorophenyl) and 3-(aminomethyl) pyrrolidine functional groups (Figs. 5ii and 7).
404 Org214444-0 has a similar oxyphenyl core, which is approximately twice as bulky due to the
405 functional groups attached to it. 9045 docked to cFSHR in a horseshoe conformation. Although it
406 interacted with L497_{cFSHR}, P498_{cFSHR} and M499_{cFSHR} on ECL2, there were many interactions
407 observed with the TM helices, e.g., with I567^{6.51}_{cFSHR} (TM6), S568^{6.52}_{cFSHR} (TM6), A571^{5.55}_{cFSHR}
408 (TM6), N517^{5.47}_{cFSHR}, and Y594^{7.42}_{cFSHR} (TM7).

cLHR-4681



409 TM1(yellow), TM2(orange), TM3(peach), TM4 (pink), TM5(teal), TM6(cyan), TM7 (violet) and ICD(with helix-8) (maroon).

410 **Fig. 9: Interactions between cLHR and Z1456504681.** The molecule has 1,3-thiazole at its core,
411 which is attached to piperidine, 2-methylphenyl and cyclopropyl sidechains. The (2-aminomethyl)
412 piperidine sidechain closely interacted with L532 and P533 on ECL2. Other key residues exposed
413 to the functional groups include M534 on ELC2, V545^{5,40}, L548^{5,43} and L549^{5,44} on TM5; F605^{6,54}
414 and I602^{6,51} on TM6; and Y629^{7,42} on TM7. The graph shows CRE-luciferase activity in response

415 to the tested molecule and recombinant carp LH as a function of concentration. The control denotes
416 to activity of the non-transfected COS 7 cell in response towards concerned ligand.

417 Various in silico mutations in the key residues A571^{6.55}_{cFSHR}, and I567^{6.51}_{cFSHR}, as well as in
418 P498_{cFSHR} and M499_{cFSHR} on the ECL2, significantly decreased the affinity and stability of the
419 cFSHR-9045 complex. When binding to cLHR, 9045 displayed a much more linear conformation
420 than upon binding to cFSHR, forming mainly hydrophobic interactions and binding deeper into
421 the binding pocket (Fig. S4). The ligand penetrated more deeply into the hydrophobic cavity as
422 compared to 8028. Similar to its docking to cFSHR, the 3-(aminomethyl) pyrrolidine functional
423 group engaged with surrounding TM helices at E468^{3.37}_{cLHR} (TM3), N552^{5.47}_{cLHR} (TM5),
424 I602^{6.51}_{cLHR} (TM6) and Y629^{7.42}_{cLHR} (TM7), which played a crucial role in post-docking
425 conformational modulation of cLHR (Fig. S5). Further, upon binding to 9045, the orientation of
426 cLHR residues I602^{6.51}_{cLHR} and N552^{5.47}_{cLHR} and cFSHR residues Y594^{7.42}_{cFSHR} and N517^{5.47}_{cFSHR}
427 in cFSHR diverged towards the ligand and internally engaged other exposed residues on the
428 surrounding TM helices. We hypothesize that these interactions of 9045 with both cFSHR and
429 cLHR substantially restrict the post-docking conformational changes, hence accounts for the lower
430 potency of the molecule.

431 The in-silico method we used to generate receptor cavity-based hypothesis and for
432 pharmacophore screening considerably increases the probability of identifying small compounds
433 capable of receptor binding and pathway-specific modulation. Though this approach has been
434 developed for efficient pharmacophore design, a few studies have tested with potential GPCR
435 modulators, and none have focused on GTHRs. Due to the elaborate activation mechanism of its
436 extracellular domain, GTHR activation through orthosteric binding of its cognate receptor is
437 elaborate and complicated. Moreover, piscine GTHR lacks the strict hormone-receptor specificity
438 seen in mammals, as both FSHR and LHR are variably promiscuous, depending on the fish species.

439 Activation can induce variable signal transduction cascades in response to the same stimulation
440 due to the large size of both receptor and hormone, which may form complexes larger than 1000
441 amino acid-long. Irregularities or mutations in these molecules may lead to various reproductive
442 disorders. Allosteric binding sites provide an alternative route for activation and modulation of
443 GTHRs, which may offer more efficient regulation of downstream signaling cascades. Screening
444 and selection of small compound modulators are expensive and time-consuming, with low return
445 of successful hits. Our in vitro analyses showed the efficiency of using a receptor cavity-based
446 hypothesis for in silico screening of small compounds with agonist effects. The molecules can be
447 further improved or turned into potential NAMs/NALs by replacing the functional groups attached
448 to the pharmacophore core. Overall, allosteric sites in GTHRs show great potential for receptor
449 manipulation while bypassing the elaborate ECD-based orthosteric activation mechanism. While
450 allosteric modulators can act in a regulatory capacity as PAMs, NAMs and NALs, they can also
451 directly manipulate the TMD independently of orthosteric mechanisms. Thus, they may be a
452 crucial tool to overcome the lack of post-binding signaling specificity seen in orthosteric GTHR
453 activation.

454 Conclusion

455 Maintaining a controlled reproductive cycle of fish is of utmost importance in aquaculture.
456 Currently, most species commonly use hormonal manipulation to regulate gonadal activity.
457 However, these hormonal treatments often have limitations, such as high costs and limited
458 effectiveness. To overcome these challenges, there is significant potential in utilizing allosteric
459 modulators as regulators of hormonal activation.

460 Our research employed the receptor cavity-based hypothesis and ligand screening method to
461 identify allosteric agonists capable of activating receptors independently from native ligands.
462 Through this approach, we successfully selected four small compounds as potential modulator

463 drug candidates for cyclic gonadotropin-releasing hormone receptors (cGTHRs). Our novel
464 pharmacophore screening procedure, which incorporated multiple in silico screening stages,
465 ADME (absorption, distribution, metabolism, and excretion) considerations, and docking results,
466 significantly enhanced the efficiency of the screening process. The efficacy of our selected
467 compounds was further confirmed through in vitro testing.

468 Considering the complexity of piscine GTHR-GTH interactions, and the significance of
469 controlling and manipulating fish reproductive cycles, our strategy holds promise for identifying
470 additional allosteric modulators. This approach has the potential to revolutionize the field of
471 aquaculture by providing cost-effective and efficient methods for regulating fish reproduction.

472 **Data and Software Availability**

473 The homology modelling structure of the inactive GnRH1R structure Were generated using I-
474 TASSER (<https://zhanggroup.org/I-TASSER/>). The template for homology modelling were
475 obtained from the Protein Data Bank (RCSB PDB: <https://www.rcsb.org/>). In this work, the site
476 map analysis, hypothesis generation, molecular docking was performed using (Maestro,
477 Schrödinger, LLC, New York, NY, 2021.) and can be downloaded from
478 <https://www.schrodinger.com/>. The compound libraries can be downloaded from
479 <https://enamine.net/compound-libraries>. The downloaded libraries were further processed and
480 used to construct conformational databases for ligands using the Phase module (Phase,
481 Schrödinger, LLC, New York, NY, 2021.) and are made available at
482 <https://zenodo.org/record/8120822> along with input files receptor homology models, docking
483 grids, and docked ligand receptor complexes. The selected compounds can be ordered from
484 Enamine online store (<https://new.enaminestore.com/>).

485

486 **AUTHOR INFORMATION**

487 **Corresponding Author**

488 *Berta Levavi-Sivan

489 Department of Animal Sciences, The Robert H. Smith Faculty of Agriculture, Food, and

490 Environment

491 Hebrew University of Jerusalem, Rehovot 76100, Israel

492 Tel: +972-8-9489988

493 E-mail: berta.sivan@mail.huji.ac.il

494 ORCID Identifier: 0000-0002-0183-9524

495 **Present Address**

496 Department of Animal Sciences, The Robert H. Smith Faculty of Agriculture, Food, and

497 Environment

498 Hebrew University of Jerusalem, Rehovot 76100, Israel

499 Tel: +972-8-9489988

500 E-mail: berta.sivan@mail.huji.ac.il

501 ORCID Identifier: 0000-0002-0183-9524

502 **Authors' contributions**

503 I.A. did the *in-silico* modelling, screening, and analysis. *In vitro* LUC assays and statistical

504 analysis were performed by L.H. H.L. ran control experiments on non-transfected cell lines. The

505 project supervision and arrangement of funding was done by B.L.S. The manuscript was written

506 through contributions of all authors. All authors have given approval to the final version of the
507 manuscript.

508 **List of Abbreviations**

509 GTH, gonadotropin; GTHR, gonadotropin receptors; cFSH, carp follicle stimulating hormone;
510 cFSHR, carp follicle stimulating hormone receptor; cLH, carp luteinizing hormone; cLHR, carp
511 luteinizing hormone receptor; LUC, luciferase activation assay; EC₅₀, half maximal effective
512 concentration.

513 **Declaration**

514 **Competing interests**

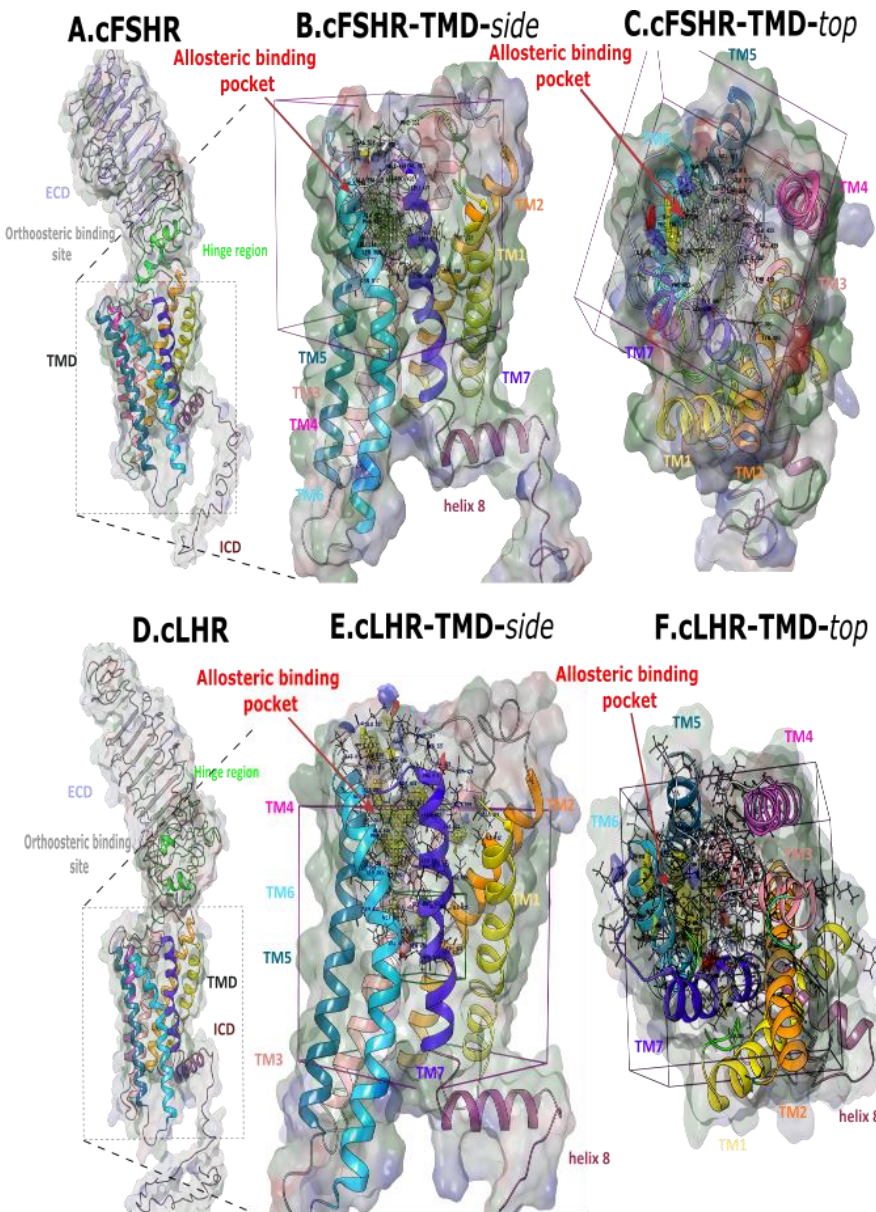
515 The authors declare that they have no conflicts of interest with the contents of this article.

516 **Funding**

517 This project has received funding from the European Union's Horizon 2020 research and
518 innovation programme under the Marie Skłodowska-Curie Grant Agreement no. 642893 –
519 IMPRESS and the USDA, NIFA-BARD Research Project IS-8339-23.

520 **Supporting Information**

521

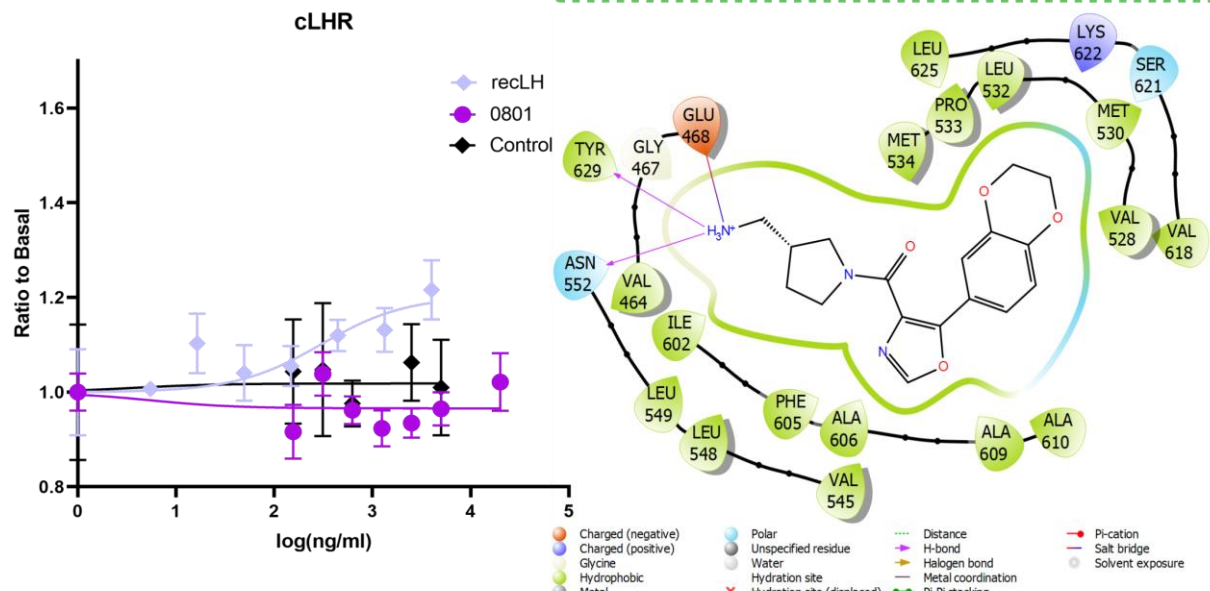
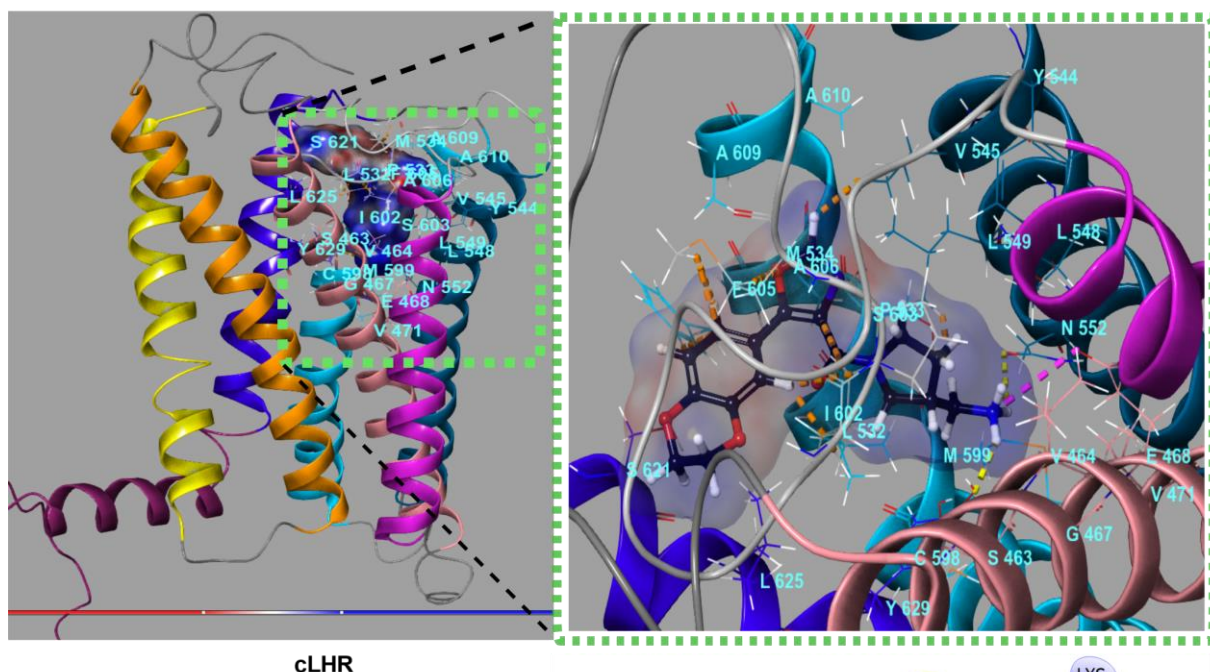


Showing cFSHR-ECD (lilac), cLHR-ECD (grey), hinge region (green), TM1(yellow), TM2(orange), TM3(peach), TM4 (pink), TM5(teal), TM6(cyan), TM7 (violet) and ICD(with helix-8) (maroon).

522

523 **Figure. S1:** Ribbon diagrams showing the targeted allosteric binding sites located within
524 hydrophobic transmembrane cavities in cFSHR (A-C) and cLHR (D-E). The transmembrane
525 regions of cFSHR are magnified in B (side view) and C (top view), and of cLHR in E (side view)
526 and F (top view).

cLHR-0801



527

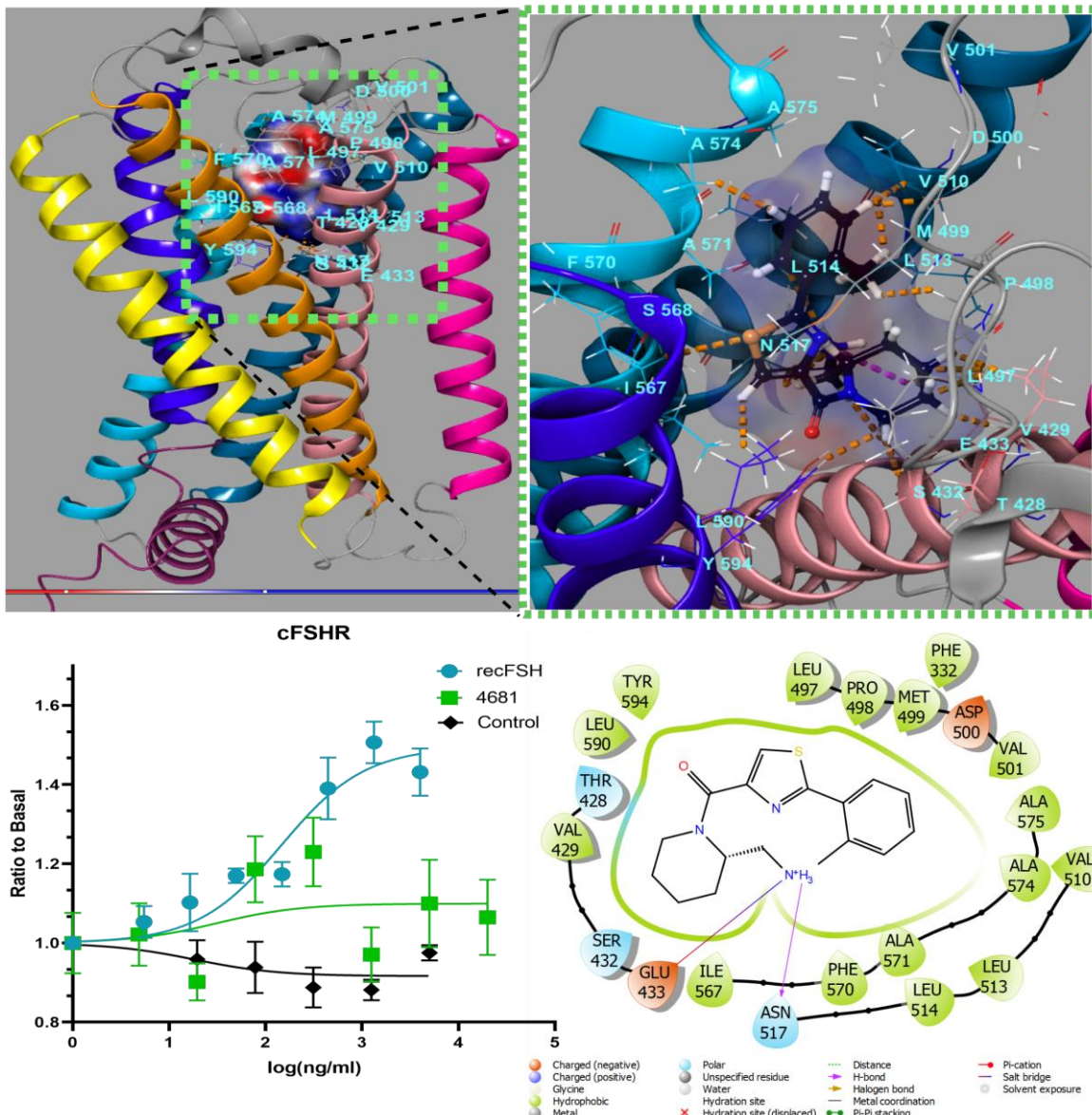
TM1(yellow), TM2(orange), TM3(peach), TM4 (pink), TM5(teal), TM6(cyan), TM7 (violet) and ICD(with helix-8) (maroon).

528
529
530
531

Figure. S2. Interactions between cLHR and Z1456630801. The graph shows CRE-luciferase activity in response to the tested molecule and recombinant ligand as a function of concentration. The control denotes to activity of the non-transfected COS 7 cell in response towards concerned ligand.

532

cFSHR-4681



533 TM1(yellow), TM2(orange), TM3(peach), TM4 (pink), TM5(teal), TM6(cyan), TM7 (violet) and ICD(with helix-8) (maroon).

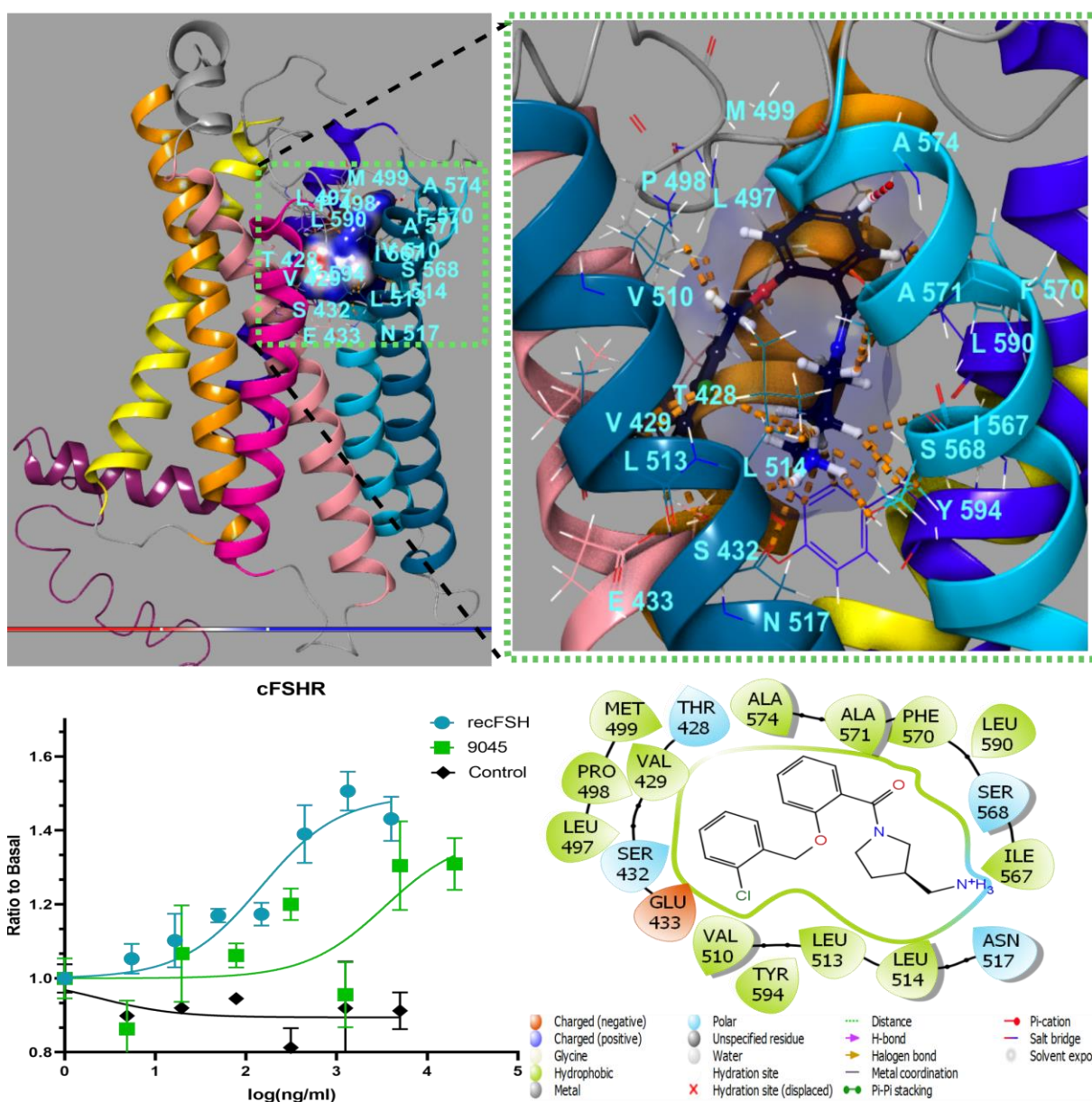
534 Fig. S3. Interactions between cFSHR and Z1456504681. The graph shows CRE-luciferase activity in
 535 response to the tested molecule and recombinant ligand as a function of concentration. The control
 536 denotes to activity of the non-transfected COS 7 cell in response towards concerned ligand.

537

538

539

cFSHR-9045

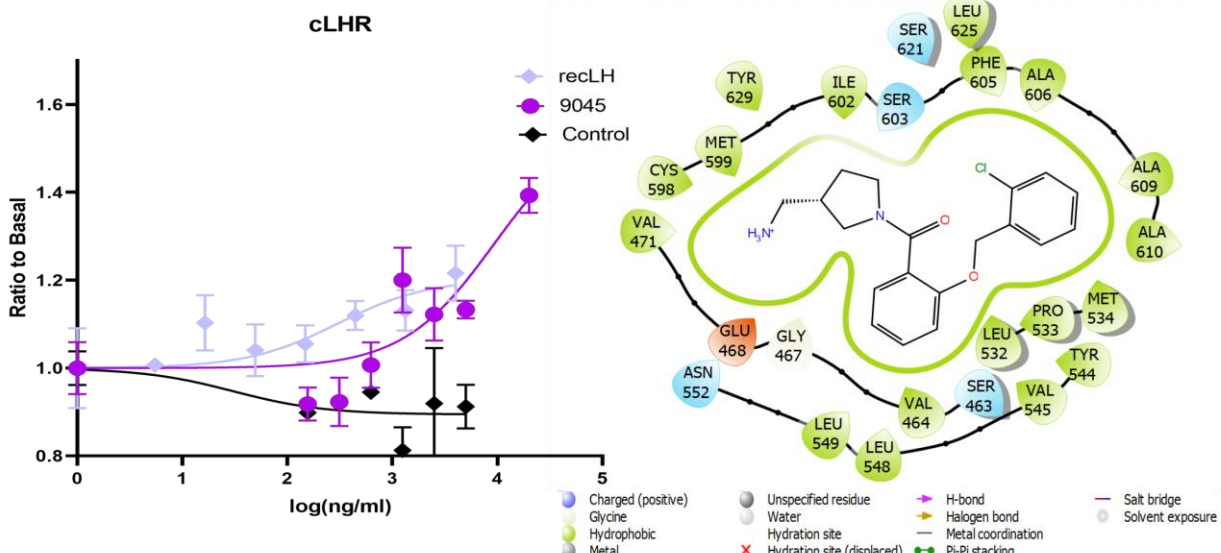
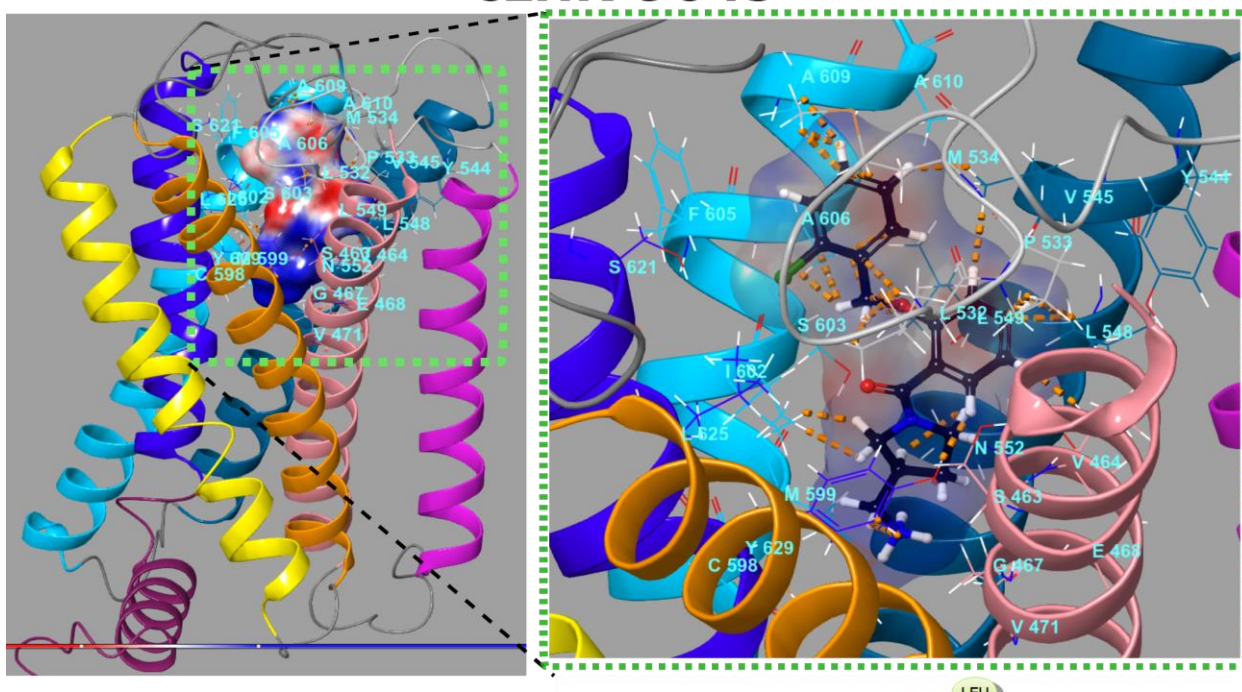


540

TM1(yellow), TM2(orange), TM3(peach), TM4 (pink), TM5(teal), TM6(cyan), TM7 (violet) and ICD(with helix-8) (maroon).

541 **Figure. S4. Interactions between cFSHR and Z2242909045.** The molecule has a methoxyphenyl core that
 542 is attached to 2-(2-chlorophenyl) and 3-(aminomethyl) pyrrolidine functional groups. The
 543 chlorophenyl group interacted with L497 and P498 on ECL2, L513^{5,43} and L514^{5,44} on TM5, and
 544 with V429^{3,33} and S432^{3,36} on TM3. The methoxyphenyl group showed associations to M499
 545 (ECL2) and the aminomethyl pyrrolidine group interacted with I567^{6,51}, S568^{6,52} and A571^{5,55}
 546 (TM6), Y594^{7,42} (TM7, internally interacts with S432^{3,36} on TM3), L514^{5,44} (TM5), and N517^{5,47}
 547 (TM5; interacts with E433^{3,37} on TM3 internally). The graph shows CRE-luciferase activity in
 548 response to the tested molecule and recombinant ligand as a function of concentration. The control
 549 denotes to activity of the non-transfected COS 7 cell in response towards concerned ligand.

cLHR-9045



550

TM1(yellow), TM2(orange), TM3(peach), TM4(pink), TM5(teal), TM6(cyan), TM7(violet) and ICD (with helix-8) (maroon).

Fig. S5. Interactions between cLHR and Z2242909045. The chlorophenyl group is exposed to ECL2 and interacts mainly with L532 and M534 and also with A606^{6,55} and A609^{6,58} (TM6). The oxyphenyl core interacts with P533 on the ECL2 and with V464^{3,33} (TM3), V545^{6,55}, L548^{5,43} and L549^{5,44} (TM5), and Y629^{7,42} (TM7). The aminomethyl pyrrolidine group interacts with I602^{6,51} (internally interacts with M599^{6,48}), N552^{5,47} (internally interacts with E468^{3,37}), and Y629^{7,42} (TM7). The graph shows CRE-luciferase activity in response to the tested molecule and recombinant ligand as a function of concentration. The control denotes to activity of the non-transfected COS 7 cell in response towards concerned ligand.

559 **References**

560 (1) Moles, G.; Hausken, K.; Carrillo, M.; Zanuy, S.; Levavi-Sivan, B.; Gomez, A. Generation and use of
561 recombinant gonadotropins in fish. *Gen Comp Endocrinol* **2020**, *299*, 113555. DOI:
562 10.1016/j.ygcn.2020.113555.

563 (2) Levavi-Sivan, B.; Bogerd, J.; Mananos, E. L.; Gomez, A.; Lareyre, J. J. Perspectives on fish
564 gonadotropins and their receptors. *Gen Comp Endocrinol* **2010**, *165* (3), 412-437. DOI:
565 10.1016/j.ygcn.2009.07.019.

566 (3) Pierce, J. G.; Parsons, T. F. Glycoprotein hormones: structure and function. *Annual review of
567 biochemistry* **1981**, *50*, 465-495. DOI: 10.1146/annurev.bi.50.070181.002341.

568 (4) Gaya, S. A.; Jennifer, J. B. Chapter 2 - Sexual Development, Growth, and Puberty in Children. In
569 *Principles of Gender-Specific Medicine (Second Edition)*, Second Edition ed.; Marianne, J. L. Ed.; Academic
570 Press, 2010; pp 18-34.

571 (5) Kitano, T.; Takenaka, T.; Takagi, H.; Yoshiura, Y.; Kazeto, Y.; Hirai, T.; Mukai, K.; Nozu, R. Roles of
572 Gonadotropin Receptors in Sexual Development of Medaka. *Cells* **2022**, *11* (3). DOI:
573 10.3390/cells11030387 From NLM Medline.

574 (6) Murozumi, N.; Nakashima, R.; Hirai, T.; Kamei, Y.; Ishikawa-Fujiwara, T.; Todo, T.; Kitano, T. Loss of
575 Follicle-Stimulating Hormone Receptor Function Causes Masculinization and Suppression of Ovarian
576 Development in Genetically Female Medaka. *Endocrinology* **2014**, *155* (8), 3136-3145. DOI:
577 10.1210/en.2013-2060.

578 (7) Duan, J.; Xu, P.; Cheng, X.; Mao, C.; Croll, T.; He, X.; Shi, J.; Luan, X.; Yin, W.; You, E.; Liu, Q.; Zhang, S.;
579 Jiang, H.; Zhang, Y.; Jiang, Y.; Xu, H. E. Structures of full-length glycoprotein hormone receptor signalling
580 complexes. *Nature* **2021**, *598* (7882), 688-692. DOI: 10.1038/s41586-021-03924-2.

581 (8) Duan, J.; Xu, P.; Zhang, H.; Luan, X.; Yang, J.; Mao, C.; Shen, D.-D.; Ji, Y.; He, X.; Cheng, X.; Jiang, H.;
582 Jiang, Y.; Zhang, S.; Zhang, Y.; Xu, H. E. Universal mechanism of hormone and allosteric agonist mediated
583 activation of glycoprotein hormone receptors as revealed by structures of follicle stimulating hormone
584 receptor. *bioRxiv* **2022**, 2022.2008.2001.502312. DOI: 10.1101/2022.08.01.502312.

585 (9) Hollander-Cohen, L.; Bohm, B.; Hausken, K.; Levavi-Sivan, B. Ontogeny of the specificity of
586 gonadotropin receptors and gene expression in carp. *Endocr Connect* **2019**, *8* (11), 1433-1446. DOI:
587 10.1530/EC-19-0389.

588 (10) Aizen, J.; Kowalsman, N.; Kobayashi, M.; Hollander, L.; Sohn, Y. C.; Yoshizaki, G.; Niv, M. Y.; Levavi-
589 Sivan, B. Experimental and computational study of inter- and intra- species specificity of gonadotropins
590 for various gonadotropin receptors. *Mol Cell Endocrinol* **2012**, *364* (1-2), 89-100. DOI:
591 10.1016/j.mce.2012.08.013.

592 (11) Atre, I.; Mizrahi, N.; Yebra-Pimentel, E. S.; Hausken, K.; Yom-Din, S.; Hurvitz, A.; Dirks, R.; Degani, G.;
593 Levavi-Sivan, B. Molecular characterization of two Russian sturgeon gonadotropin receptors: Cloning,
594 expression analysis, and functional activity. *Gen Comp Endocrinol* **2020**, *298*, 113557. DOI:
595 10.1016/j.ygcn.2020.113557.

596 (12) Burow, S.; Fontaine, R.; von Krogh, K.; Mayer, I.; Nourizadeh-Lillabadi, R.; Hollander-Cohen, L.;
597 Cohen, Y.; Shpilman, M.; Levavi-Sivan, B.; Weltzien, F. A. Data on Western blot and ELISA analysis of
598 medaka (*Oryzias latipes*) follicle-stimulating hormone (Fsh) and luteinizing hormone (Lh) using
599 recombinant proteins expressed with *Pichia pastoris*. *Data in brief* **2019**, *22*, 1057-1063. DOI:
600 10.1016/j.dib.2019.01.034.

601 (13) Brüser, A.; Schulz, A.; Rothemund, S.; Ricken, A.; Calebiro, D.; Kleinau, G.; Schöneberg, T. The
602 Activation Mechanism of Glycoprotein Hormone Receptors with Implications in the Cause and Therapy
603 of Endocrine Diseases. *Journal of Biological Chemistry* **2016**, *291* (2), 508-520. DOI:
604 10.1074/jbc.M115.701102.

605 (14) Shpakov, A. Allosteric Modulators of G Protein-Coupled Receptors. *Int J Mol Sci* **2022**, *23* (6). DOI: 10.3390/ijms23062934.

606 (15) Landomiel, F.; De Pascali, F.; Raynaud, P.; Jean-Alphonse, F.; Yvinec, R.; Pellissier, L. P.; Bozon, V.; Bruneau, G.; Crepieux, P.; Poupon, A.; Reiter, E. Biased Signaling and Allosteric Modulation at the FSHR. *Frontiers in endocrinology* **2019**, *10*, 148. DOI: 10.3389/fendo.2019.00148 From NLM PubMed-not-MEDLINE.

607 (16) Anderson, R. C.; Newton, C. L.; Millar, R. P. Small Molecule Follicle-Stimulating Hormone Receptor Agonists and Antagonists. *Frontiers in endocrinology* **2018**, *9*, 757. DOI: 10.3389/fendo.2018.00757 From NLM PubMed-not-MEDLINE.

608 (17) Nataraja, S. G.; Yu, H. N.; Palmer, S. S. Discovery and Development of Small Molecule Allosteric Modulators of Glycoprotein Hormone Receptors. *Frontiers in endocrinology* **2015**, *6*, 142. DOI: 10.3389/fendo.2015.00142 From NLM PubMed-not-MEDLINE.

609 (18) Slosky, L. M.; Caron, M. G.; Barak, L. S. Biased Allosteric Modulators: New Frontiers in GPCR Drug Discovery. *Trends Pharmacol Sci* **2021**, *42* (4), 283-299. DOI: 10.1016/j.tips.2020.12.005 From NLM Medline.

610 (19) Yanofsky, S. D.; Shen, E. S.; Holden, F.; Whitehorn, E.; Aguilar, B.; Tate, E.; Holmes, C. P.; Scheuerman, R.; MacLean, D.; Wu, M. M.; Frail, D. E.; Lopez, F. J.; Winneker, R.; Arey, B. J.; Barrett, R. W. Allosteric activation of the follicle-stimulating hormone (FSH) receptor by selective, nonpeptide agonists. *The Journal of biological chemistry* **2006**, *281* (19), 13226-13233. DOI: 10.1074/jbc.M600601200 From NLM Medline.

611 (20) Wrobel, J.; Jetter, J.; Kao, W.; Rogers, J.; Di, L.; Chi, J.; Perez, M. C.; Chen, G. C.; Shen, E. S. 5-Alkylated thiazolidinones as follicle-stimulating hormone (FSH) receptor agonists. *Bioorg Med Chem* **2006**, *14* (16), 5729-5741. DOI: 10.1016/j.bmc.2006.04.012 From NLM Medline.

612 (21) Derkach, K. V.; Romanova, I. V.; Bakhtyukov, A. A.; Morina, I. Y.; Dar'in, D. V.; Sorokoumov, V. N.; Shpakov, A. O. The Effect of Low-Molecular-Weight Allosteric Agonist of Luteinizing Hormone Receptor on Functional State of the Testes in Aging and Diabetic Rats. *Bull Exp Biol Med* **2021**, *171* (1), 81-86. DOI: 10.1007/s10517-021-05177-5 From NLM Medline.

613 (22) van Koppen, C. J.; Zaman, G. J.; Timmers, C. M.; Kelder, J.; Mosselman, S.; van de Lagemaat, R.; Smit, M. J.; Hanssen, R. G. A signaling-selective, nanomolar potent allosteric low molecular weight agonist for the human luteinizing hormone receptor. *Naunyn Schmiedebergs Arch Pharmacol* **2008**, *378* (5), 503-514. DOI: 10.1007/s00210-008-0318-3 From NLM Medline.

614 (23) Lu, S.; Zhang, J. Small Molecule Allosteric Modulators of G-Protein-Coupled Receptors: Drug-Target Interactions. *J Med Chem* **2019**, *62* (1), 24-45. DOI: 10.1021/acs.jmedchem.7b01844.

615 (24) Dixon, S. L.; Smolyrev, A. M.; Knoll, E. H.; Rao, S. N.; Shaw, D. E.; Friesner, R. A. PHASE: a new engine for pharmacophore perception, 3D QSAR model development, and 3D database screening: 1. Methodology and preliminary results. *J Comput Aided Mol Des* **2006**, *20* (10-11), 647-671. DOI: 10.1007/s10822-006-9087-6.

616 (25) Friesner, R. A.; Murphy, R. B.; Repasky, M. P.; Frye, L. L.; Greenwood, J. R.; Halgren, T. A.; Sanschagrin, P. C.; Mainz, D. T. Extra precision glide: docking and scoring incorporating a model of hydrophobic enclosure for protein-ligand complexes. *J Med Chem* **2006**, *49* (21), 6177-6196. DOI: 10.1021/jm051256o.

617 (26) Biran, J.; Ben-Dor, S.; Levavi-Sivan, B. Molecular identification and functional characterization of the kisspeptin/kisspeptin receptor system in lower vertebrates. *Biology of reproduction* **2008**, *79* (4), 776-786. DOI: 10.1095/biolreprod.107.066266.

618 (27) Levavi-Sivan, B.; Aizen, J.; Avitan, A. Cloning, characterization and expression of the D2 dopamine receptor from the tilapia pituitary. *Molecular and Cellular Endocrinology* **2005**, *236* (1-2), 17-30.

619 (28) Tallarida, R. J.; Murray, R. B. Relative Potency I. In *Manual of Pharmacologic Calculations: With Computer Programs*, Tallarida, R. J., Murray, R. B. Eds.; Springer New York, 1987; pp 35-38.

653 (29) Duan, J.; Xu, P.; Zhang, H.; Luan, X.; Yang, J.; He, X.; Mao, C.; Shen, D. D.; Ji, Y.; Cheng, X.; Jiang, H.;
654 Jiang, Y.; Zhang, S.; Zhang, Y.; Xu, H. E. Mechanism of hormone and allosteric agonist mediated
655 activation of follicle stimulating hormone receptor. *Nat Commun* **2023**, *14* (1), 519. DOI:
656 10.1038/s41467-023-36170-3 From NLM Medline.

657 (30) Gether, U. Uncovering molecular mechanisms involved in activation of G protein-coupled receptors.
658 *Endocrine reviews* **2000**, *21* (1), 90-113. DOI: 10.1210/edrv.21.1.0390.

659 (31) Vassart, G.; Pardo, L.; Costagliola, S. A molecular dissection of the glycoprotein hormone receptors.
660 *Trends in biochemical sciences* **2004**, *29* (3), 119-126. DOI: 10.1016/j.tibs.2004.01.006.

661 (32) Arey, B. J. Allosteric modulators of glycoprotein hormone receptors: discovery and therapeutic
662 potential. *Endocrine* **2008**, *34* (1-3), 1-10. DOI: 10.1007/s12020-008-9098-2.

663 (33) Heitman, L. H.; Oosterom, J.; Bonger, K. M.; Timmers, C. M.; Wiegerinck, P. H.; Ijzerman, A. P.
664 [³H]Org 43553, the first low-molecular-weight agonistic and allosteric radioligand for the human
665 luteinizing hormone receptor. *Mol Pharmacol* **2008**, *73* (2), 518-524. DOI: 10.1124/mol.107.039875
666 From NLM Medline.

667 (34) Banerjee, A. A.; Mahale, S. D. Role of the Extracellular and Intracellular Loops of Follicle-Stimulating
668 Hormone Receptor in Its Function. *Frontiers in endocrinology* **2015**, *6*, 110. DOI:
669 10.3389/fendo.2015.00110 From NLM PubMed-not-MEDLINE.

670 (35) Meduri, G.; Touraine, P.; Beau, I.; Lahuna, O.; Desroches, A.; Vacher-Lavenu, M. C.; Kuttenn, F.;
671 Misrahi, M. Delayed puberty and primary amenorrhea associated with a novel mutation of the human
672 follicle-stimulating hormone receptor: clinical, histological, and molecular studies. *J Clin Endocrinol
673 Metab* **2003**, *88* (8), 3491-3498. DOI: 10.1210/jc.2003-030217 From NLM Medline.

674 (36) Li, S.; Liu, X.; Min, L.; Ascoli, M. Mutations of the second extracellular loop of the human lutropin
675 receptor emphasize the importance of receptor activation and de-emphasize the importance of receptor
676 phosphorylation in agonist-induced internalization. *The Journal of biological chemistry* **2001**, *276* (11),
677 7968-7973. DOI: 10.1074/jbc.M010482200 From NLM Medline.

678

679

680

681

682

683

684

685

686

687

688

689

For Table of Contents Use Only

Receptor cavity-based screening reveals potential allosteric modulators of gonadotropin receptors in carp (*Cyprinus carpio*).

Ishwar Atre, Lian Hollander-Cohen, Berta Levavi-Sivan*

